

RankSEG: A Consistent Ranking-based Framework for Segmentation

Ben Dai

BENDAI@CUHK.EDU.HK

Department of Statistics
The Chinese University of Hong Kong
Hong Kong SAR

Chunlin Li

LI000007@UMN.EDU

School of Statistics
University of Minnesota
MN 55455 USA

Abstract

Segmentation has emerged as a fundamental field of computer vision and natural language processing, which assigns a label to every pixel/feature to extract regions of interest from an image/text. To evaluate the performance of segmentation, the Dice and IoU metrics are used to measure the degree of overlap between the ground truth and the predicted segmentation. In this paper, we establish a theoretical foundation of segmentation with respect to the Dice/IoU metrics, including the Bayes rule and Dice/IoU-calibration, analogous to classification-calibration or Fisher consistency in classification. We prove that the existing thresholding-based framework with most operating losses are not consistent with respect to the Dice/IoU metrics, and thus may lead to a suboptimal solution. To address this pitfall, we propose a novel consistent ranking-based framework, namely *RankDice/RankIoU*, inspired by plug-in rules of the Bayes segmentation rule. Three numerical algorithms with GPU parallel execution are developed to implement the proposed framework in large-scale and high-dimensional segmentation. We study statistical properties of the proposed framework. We show it is Dice-/IoU-calibrated, and its excess risk bounds and the rate of convergence are also provided. The numerical effectiveness of *RankDice/mRankDice* is demonstrated in various simulated examples and *Fine-annotated CityScapes* and *Pascal VOC* datasets with state-of-the-art deep learning architectures.

Keywords: Segmentation, Bayes rule, ranking, Dice-calibrated, excess risk bounds, Poisson-binomial distribution, normal approximation, GPU computing

1. Introduction

Segmentation is one of the key tasks in the field of computer vision and natural language processing, which groups together similar pixels/features of an input that belong to the same class (Ronneberger et al., 2015; Badrinarayanan et al., 2017). It has become an essential part of image and text understanding with applications in autonomous vehicles (Assidiq et al., 2008), medical image diagnostics (Wang et al., 2018), face/fingerprint recognition (Xin et al., 2018), and video action localization (Shou et al., 2017).

The primary aim of segmentation is to label each foreground feature/pixel of an input with a corresponding class. Specifically, for a feature vector or an image $\mathbf{X} \in \mathbb{R}^d$, a *segmentation function* $\boldsymbol{\delta} : \mathbb{R}^d \rightarrow \{0, 1\}^d$ yields a predicted segmentation $\boldsymbol{\delta}(\mathbf{X}) = (\delta_1(\mathbf{X}), \dots, \delta_d(\mathbf{X}))^\top$, where $\delta_j(\mathbf{X})$ represents the predicted segmentation for the j -th feature X_j , and $I(\boldsymbol{\delta}(\mathbf{X})) = \{j : \delta_j(\mathbf{X}) = 1; \text{ for } j = 1, \dots, d\}$ is the index set of the segmented features of \mathbf{X} provided by $\boldsymbol{\delta}$. Correspondingly, $\mathbf{Y} \in \{0, 1\}^d$ is a feature-wise label of a ground truth segmentation, where $Y_j = 1$ indicates that the j -th feature/pixel

X_j is segmented, and $I(\mathbf{Y}) = \{j : \mathbf{Y}_j = 1; \text{ for } j = 1, \dots, d\}$ is the index set of the ground-truth features.

To access the performance for a segmentation function δ , the Dice and IoU metrics are introduced and widely used in the literature (Milletari et al., 2016), both of which measure the overlap between the ground truth and the predicted segmentation:

$$\begin{aligned} \text{Dice}_\gamma(\delta) &= \mathbb{E} \left(\frac{2|I(\mathbf{Y}) \cap I(\delta(\mathbf{X}))| + \gamma}{|I(\mathbf{Y})| + |I(\delta(\mathbf{X}))| + \gamma} \right) = \mathbb{E} \left(\frac{2\mathbf{Y}^\top \delta(\mathbf{X}) + \gamma}{\|\mathbf{Y}\|_1 + \|\delta(\mathbf{X})\|_1 + \gamma} \right), \\ \text{IoU}_\gamma(\delta) &= \mathbb{E} \left(\frac{|I(\mathbf{Y}) \cap I(\delta(\mathbf{X}))| + \gamma}{|I(\mathbf{Y}) \cup I(\delta(\mathbf{X}))| + \gamma} \right) = \mathbb{E} \left(\frac{\mathbf{Y}^\top \delta(\mathbf{X}) + \gamma}{\|\mathbf{Y}\|_1 + \|\delta(\mathbf{X})\|_1 - \mathbf{Y}^\top \delta(\mathbf{X}) + \gamma} \right). \end{aligned} \quad (1)$$

where $|\cdot|$ is the cardinality of a set, and $\gamma \geq 0$ is a smoothing parameter. When $\gamma = 0$, $\text{Dice}_\gamma(\delta) = \mathbb{E}(2\text{TP}/(2\text{TP} + \text{FP} + \text{FN}))$, $\text{IoU}_\gamma(\delta) = \mathbb{E}(\text{TP}/(\text{TP} + \text{FP} + \text{FN}))$ where TP is the true positive, FP is the false positive, and FN is the false negative. We postpone the discussion on the relationship between the Dice and IoU metrics in Section 4.2. For clarity of presentation, we focus on the Dice metric in the sequel, and discuss the extensibility to the IoU metric in Section 4.2.

The recent success of fully convolutional networks has enabled significant progress in segmentation. In literature, the mainstream of recent works devoted to designing and developing neural network architectures under different segmentation scenarios, including FCN (Long et al., 2015), U-Net (Ronneberger et al., 2015), DeepLab (Chen et al., 2018), and PSPNet (Zhao et al., 2017). Despite their remarkable performance, most existing models are fitted to provide prediction under a framework that treats segmentation as classification, completely ignoring their innate differences (as discussed in Section 1.1). We find this framework leading to an inconsistent solution and sub-optimal performance with respect to the Dice/IoU metrics, and we address this pitfall by developing a novel consistent ranking-based framework, namely *RankSEG* (*RankDice* to the Dice metric and *RankIoU* to the IoU metric), to further improve the segmentation performance.

1.1 Existing methods

Most existing segmentation methods are developed under a threshold-based framework with two types of loss functions.

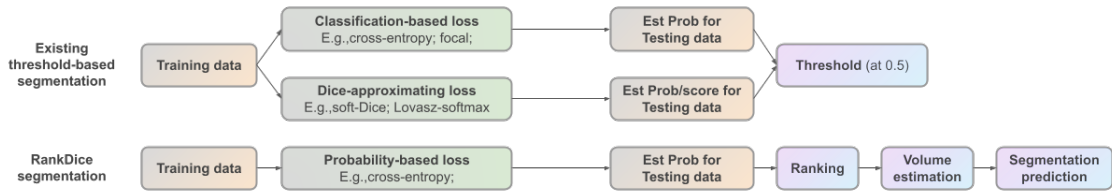


Figure 1: The existing and the proposed (*RankDice*) frameworks for segmentation. The upper panel is the existing *threshold-based segmentation* framework, and the lower panel is the proposed *RankDice* framework.

As indicated in Figure 1, the existing threshold-based segmentation framework, inspired by binary classification, provides a predicted segmentation via a two-stage procedure: (i) estimating

a decision function or a probability function based on a loss; (ii) predicting feature-wise labels by thresholding the estimated decision function or probabilities. Specifically, given a training dataset $(\mathbf{x}_i, \mathbf{y}_i)_{i=1}^n$, the prediction provided by the threshold-based framework for a new instance \mathbf{x} can be formulated as:

$$\hat{\mathbf{q}} = \operatorname{argmin}_{\mathbf{q} \in \mathcal{Q}} \frac{1}{n} \sum_{i=1}^n l(\mathbf{y}_i, \mathbf{q}(\mathbf{x}_i)) + \lambda \|\mathbf{q}\|^2, \quad \hat{\boldsymbol{\delta}}(\mathbf{x}) = \mathbf{1}(\hat{\mathbf{q}}(\mathbf{x}) \geq 0.5), \quad (2)$$

where $l(\cdot, \cdot)$ is an operating loss, $\mathbf{q} : \mathbb{R}^d \rightarrow [0, 1]^d$ is a candidate probability function with q_j being the candidate probability of the j -th pixel, \mathcal{Q} is a class of candidate probability functions, $\|\mathbf{q}\|$ is a regularization term, $\lambda > 0$ is a tuning parameter to balance the overfitting and underfitting, and $\mathbf{1}(\cdot)$ is an indicator function. For ease of presentation, $q_j(\mathbf{x})$ is specified as a probability function and a predicted segmentation is produced by thresholding at 0.5, yet it can be equally extended to a general decision function. For example, we may formulate $q_j(\mathbf{x})$ as a decision function with range in \mathbb{R} , and the prediction is produced by thresholding at 0, analogous to SVMs in classification (Cortes and Vapnik, 1995). Next, under the framework (2), two different types of operating loss functions are considered, namely the *classification-based losses* and the *Dice-approximating losses*. **Classification-based losses** completely characterize segmentation as a classification problem, with examples such as the cross-entropy (CE; Cox (1958)) and the focal loss (Focal; Lin et al. (2017)):

$$(\text{CE}) \quad l_{\text{CE}}(\mathbf{y}, \mathbf{q}(\mathbf{x})) = - \sum_{j=1}^d \left(y_j \log(\mathbf{q}_j(\mathbf{x})) + (1 - y_j) \log(1 - \mathbf{q}_j(\mathbf{x})) \right), \quad (3)$$

$$(\text{Focal}) \quad l_{\text{focal}}(\mathbf{y}, \mathbf{q}(\mathbf{x})) = - \sum_{j=1}^d \left(y_j (1 - \mathbf{q}_j(\mathbf{x}))^{\vartheta} \log(\mathbf{q}_j(\mathbf{x})) + (1 - y_j) \mathbf{q}_j^{\vartheta}(\mathbf{x}) \log(1 - \mathbf{q}_j(\mathbf{x})) \right),$$

where $\vartheta \geq 0$ is a hyperparameter for the focal loss (Lin et al., 2017). Other margin-based losses such as the hinge loss, in principle, can be included as classification-based losses with a decision function ranged in \mathbb{R} thresholding at 0, although they are less frequently used in a multiclass problem (Tewari and Bartlett, 2007). Therefore, we focus on the probability-based classification loss in the sequel.

Dice-approximating losses aim to approximate the Dice/IoU metric and conduct a direct optimization. Typical examples are the soft-Dice (Sudre et al., 2017) and the Lovasz-softmax loss (Berman et al., 2018):

$$\begin{aligned} (\text{Soft-Dice}) \quad l_{\text{SoftD}}(\mathbf{y}, \mathbf{q}(\mathbf{x})) &= 1 - \frac{2\mathbf{y}^T \mathbf{q}(\mathbf{x})}{\|\mathbf{y}\|_1 + \|\mathbf{q}(\mathbf{x})\|_1}, \\ (\text{Lovasz-softmax}) \quad l_{\text{l-softmax}}(\mathbf{y}, \mathbf{q}(\mathbf{x})) &= \bar{V}(\mathbf{y} \circ (1 - \mathbf{q}(\mathbf{x})) + (1 - \mathbf{y}) \circ \mathbf{q}(\mathbf{x})), \end{aligned}$$

where $\bar{V}(\cdot)$ is the Lovasz extension of the mis-IoU error (Berman et al., 2018), and \circ is the element-wise product. Specifically, the soft-Dice loss replaces the binary segmentation indicator $\boldsymbol{\delta}(\mathbf{x}) \in \{0, 1\}^d$ in the Dice metric by a candidate probability function $\mathbf{q}(\mathbf{x}) \in [0, 1]^d$ to make the computation feasible. The Lovasz-softmax directly takes a convex extension of IoU based on a softmax transformation. Moreover, other losses including the Tversky loss (Salehi et al., 2017), the Lovasz-hinge loss (Berman et al., 2018), and the log-Cosh Dice loss (Jadon, 2021) can be also categorized as Dice-approximating losses.

Although the existing methods based the threshold-based framework in (2) with a classification-based loss or a Dice-approximating loss are widely used in segmentation prediction, and deliver

encouraging performance in real applications, we show that the minimizer from (2) (based on the cross-entropy, the soft-Dice and the focal loss) is **inconsistent** (or sub-optimal) to the Dice metric, see Lemma 8. For Lovasz convex losses, it is still unclear if they are able to yield an optimal segmentation (convex closure is usually not enough to ensure the consistency (Bartlett et al., 2006)). Moreover, in practice, only a small number of pixel predictions are taken into account in one stochastic gradient step. Therefore, the Lovasz-softmax loss cannot directly optimize the segmentation metric (see Section 3.1 in Berman et al. (2018)). Taken together, the currently dominant framework (2) with existing losses may yield a sub-optimal solution, demanding efforts to further improve the performance, robustness and sustainability of the existing segmentation framework.

1.2 Our contribution

In this paper, we propose a novel Dice-calibrated ranking-based segmentation framework, namely *RankDice*, to address the inconsistency of the existing framework. *RankDice* is primarily inspired by the Bayes rule of Dice-segmentation. We summarize our major contribution as follows:

1. To our best knowledge, the proposed ranking-based segmentation framework *RankDice*, is the first consistent segmentation framework with respect to the Dice metric (Dice-calibrated).
2. Three numerical algorithms with GPU parallel execution are developed to implement the proposed framework in large-scale and high-dimensional segmentation.
3. We establish a theoretical foundation of segmentation with respect to the Dice metric, such as the Bayes rule and Dice-calibration. Moreover, we present Dice-calibrated consistency (Lemma 9) and a convergence rate of the excess risk (Theorem 10) for the proposed *RankDice* framework, and indicate inconsistent results for the existing methods (Lemma 8).
4. Our experiments in two simulated examples and two real datasets (CityScapes dataset and Pascal VOC 2021 dataset) suggest that the improvement of *RankDice* over the existing framework is practically significant for various loss functions and network architectures (see Tables 2-6).

It is worth noting that the results are equally applicable to the proposed *RankIoU* framework in terms of the IoU metric.

2. RankDice

It is reasonable to assume that all information on a feature-wise label is solely based on input features, that is, $Y_i \perp Y_j | \mathbf{X}$ for any $i \neq j$. Without loss of generality, we further assume that $p_j(\mathbf{X}) := \mathbb{P}(Y_j = 1 | \mathbf{X})$ are distinct for $j = 1, \dots, d$ with probability one.

2.1 Bayes segmentation rule

To begin with, we call segmentation with respect to the Dice metric as ‘‘Dice-segmentation’’. Then, we discuss Dice-segmentation at the population level, and present its Bayes (optimal) segmentation rule in Theorem 1 akin to the Bayes classifier for classification.

Theorem 1 (The Bayes rule for Dice-segmentation) A segmentation rule δ^* is a global maximizer of $\text{Dice}_\gamma(\delta)$ if and only if it satisfies that

$$\delta_j^*(\mathbf{x}) = \begin{cases} 1 & \text{if } p_j(\mathbf{x}) \text{ ranks top } \tau^*(\mathbf{x}), \\ 0 & \text{otherwise.} \end{cases}$$

The optimal volume $\tau^*(\mathbf{x})$ is given as

$$\tau^*(\mathbf{x}) = \underset{\tau \in \{0,1,\dots,d\}}{\text{argmax}} \left(\sum_{j \in J_\tau(\mathbf{x})} \sum_{l=0}^{d-1} \frac{2}{\tau + l + \gamma + 1} p_j(\mathbf{x}) \mathbb{P}(\Gamma_{-j}(\mathbf{x}) = l) + \sum_{l=0}^d \frac{\gamma}{\tau + l + \gamma} \mathbb{P}(\Gamma(\mathbf{x}) = l) \right), \quad (4)$$

where $J_\tau(\mathbf{x}) = \{j : \sum_{j'=1}^d \mathbf{1}(p_{j'}(\mathbf{x}) \geq p_j(\mathbf{x})) \leq \tau\}$ is the index set of the τ -largest conditional probabilities with $J_0(\mathbf{x}) = \emptyset$, $\Gamma(\mathbf{x}) = \sum_{j=1}^d B_j(\mathbf{x})$, and $\Gamma_{-j}(\mathbf{x}) = \sum_{j' \neq j} B_{j'}(\mathbf{x})$ are Poisson-binomial random variables, and $B_j(\mathbf{x})$ is a Bernoulli random variable with the success probability $p_j(\mathbf{x})$. See the definition of the Poisson-binomial distribution in Appendix B.3.

Two remarkable observations emerge from Theorem 1. First, the Bayes segmentation operator can be obtained via a two-stage procedure: (i) ranking the conditional probability $p_j(\mathbf{x})$, and (ii) searching for the optimal volume of the segmented features $\tau(\mathbf{x})$. Second, both the Bayes segmentation rule $\delta^*(\mathbf{x})$ and the optimal volume function $\tau^*(\mathbf{x})$ are achievable when the conditional probability $\mathbf{p}(\mathbf{x}) = (p_1(\mathbf{x}), \dots, p_d(\mathbf{x}))^\top$ is well-estimated. Therefore, our proposed framework *RankDice* is directly inspired by a general *plug-in rule* of the Bayes segmentation rule.

Moreover, the Bayes rule for Dice-segmentation is unlikely to be obtained by a fixed thresholding. Lemma 8 confirms this fact that the soft-Dice, the cross-entropy loss, the focal loss, and even a general classification-calibrated loss (Zhang, 2004; Bartlett et al., 2006), are not Dice-calibrated. See the definition of Dice-calibrated (Definition 7), the negative results for existing methods (Lemma 8), and more discussion in Section 4.1. Besides, the Bayes rule for IoU-segmentation is presented in Lemma 12.

2.2 Proposed framework

Suppose a training dataset $(\mathbf{x}_i, \mathbf{y}_i)_{i=1}^n$ is given, where $\mathbf{x}_i \in \mathbb{R}^d$ and $\mathbf{y}_i \in \{0,1\}^d$ are the input features and the true label for the i -th instance. Inspired by Theorem 1, we develop a ranking-based framework *RankDice* for Dice-segmentation (Steps 1-3).

Step 1 (Conditional probability estimation): Estimate the conditional probability based on logistic regression (the cross-entropy loss):

$$\hat{\mathbf{q}}(\mathbf{x}) = \underset{\mathbf{q} \in \mathcal{Q}}{\text{argmin}} - \sum_{i=1}^n \sum_{j=1}^d \left(y_{ij} \log(q_j(\mathbf{x}_i)) + (1 - y_{ij}) \log(1 - q_j(\mathbf{x}_i)) \right) + \lambda \|\mathbf{q}\|^2, \quad (5)$$

where \mathcal{Q} is a class of candidate probability functions, $\|\mathbf{q}\|$ is a regularization for a candidate function, and $\lambda > 0$ is a hyperparameter to balance the loss and regularization. For example, $\mathbf{q} \in \mathcal{Q}$ is usually a deep convolutional neural network for image segmentation, and $\|\mathbf{q}\|$ can be a matrix norm of weight matrices in the network.

Step 2 (Ranking): Given a new instance \mathbf{x} , rank its estimated conditional probabilities decreasingly, and denote the corresponding indices as j_1, \dots, j_d , that is, $\hat{q}_{j_1}(\mathbf{x}) \geq \hat{q}_{j_2}(\mathbf{x}) \geq \dots \geq \hat{q}_{j_d}(\mathbf{x})$.

Step 3 (Volume estimation): From (4), we estimate the volume $\hat{\tau}(\mathbf{x})$ by replacing the true conditional probability $\mathbf{p}(\mathbf{x})$ by the estimated one $\hat{\mathbf{q}}(\mathbf{x})$:

$$\hat{\tau}(\mathbf{x}) = \operatorname{argmax}_{\tau \in \{0, \dots, d\}} \sum_{s=1}^{\tau} \sum_{l=0}^{d-1} \frac{2}{\tau + l + \gamma + 1} \hat{q}_{js}(\mathbf{x}) \mathbb{P}(\hat{\Gamma}_{-js}(\mathbf{x}) = l) + \sum_{l=0}^d \frac{\gamma}{\tau + l + \gamma} \mathbb{P}(\hat{\Gamma}(\mathbf{x}) = l), \quad (6)$$

where $\hat{\Gamma}(\mathbf{x}) = \sum_{j=1}^d \hat{B}_j(\mathbf{x})$ and $\hat{\Gamma}_{-js}(\mathbf{x}) = \sum_{j \neq js} \hat{B}_j(\mathbf{x})$ are Poisson-binomial random variables, and $\hat{B}_j(\mathbf{x})$ are independent Bernoulli random variables with success probabilities $\hat{q}_j(\mathbf{x})$; for $j = 1, \dots, d$.

Finally, the predicted segmentation $\hat{\boldsymbol{\delta}}(\mathbf{x}) = (\hat{\delta}_1(\mathbf{x}), \dots, \hat{\delta}_d(\mathbf{x}))^\top$ is given by selecting the indices of the top- $\hat{\tau}(\mathbf{x})$ conditional probabilities:

$$\hat{\delta}_j(\mathbf{x}) = 1, \text{ if } j \in \{j_1, \dots, j_{\hat{\tau}(\mathbf{x})}\}; \quad \hat{\delta}_j(\mathbf{x}) = 0, \text{ otherwise.} \quad (7)$$

The proposed *RankDice* framework (Steps 1 - 3) provides a feasible solution to the Bayes segmentation rule in terms of the Dice metric. Note that **Step 1** is a standard conditional probability estimation, and **Step 2** simply ranks the estimated conditional probabilities. Next, we focus on developing a scalable computing scheme for **Step 3**.

2.3 Scalable computing schemes

This section develops scalable computing schemes for *volume estimation* in (6). Note that (6) can be rewritten as:

$$\begin{aligned} \hat{\tau}(\mathbf{x}) &= \operatorname{argmax}_{\tau \in \{0, \dots, d\}} \bar{\pi}_\tau(\mathbf{x}); \quad \bar{\pi}_\tau(\mathbf{x}) = \bar{\omega}_\tau(\mathbf{x}) + \bar{\nu}_\tau(\mathbf{x}), \\ \bar{\omega}_\tau(\mathbf{x}) &= \sum_{l=0}^{d-1} \frac{2\omega_{\tau,l}(\mathbf{x})}{\tau + l + \gamma + 1}, \quad \omega_{\tau,l}(\mathbf{x}) = \sum_{s=1}^{\tau} \hat{q}_{js}(\mathbf{x}) \mathbb{P}(\hat{\Gamma}_{-js}(\mathbf{x}) = l), \quad \bar{\nu}_\tau(\mathbf{x}) = \sum_{l=0}^d \frac{\gamma \mathbb{P}(\hat{\Gamma}(\mathbf{x}) = l)}{\tau + l + \gamma}. \end{aligned} \quad (8)$$

The computational complexity of solving (8) is intimately related to the dimension of input features. Therefore, we develop numerical algorithms for low- and high-dimensional segmentation separately.

2.3.1 EXACT ALGORITHMS FOR LOW-DIMENSIONAL SEGMENTATION

Exact algorithm based on FFT. When the dimension is low ($d \leq 500$), we consider an exact algorithm to evaluate $\bar{\omega}_\tau$ and $\bar{\nu}_\tau$. According to the definition of $\omega_{\tau,l}$, it can be computed by the following recursive formula ($\tau = 1, \dots, d$):

$$\boldsymbol{\omega}_\tau(\mathbf{x}) = \boldsymbol{\omega}_{\tau-1}(\mathbf{x}) + \hat{q}_{j_\tau}(\mathbf{x}) (\mathbb{P}(\hat{\Gamma}_{-j_\tau}(\mathbf{x}) = 0), \dots, \mathbb{P}(\hat{\Gamma}_{-j_\tau}(\mathbf{x}) = d-1))^\top, \quad \boldsymbol{\omega}_0(\mathbf{x}) = \mathbf{0}, \quad (9)$$

where $\boldsymbol{\omega}_\tau(\mathbf{x}) = (\omega_{\tau,0}(\mathbf{x}), \dots, \omega_{\tau,d-1}(\mathbf{x}))^\top$. On this ground, it suffices to evaluate $\mathbb{P}(\hat{\Gamma}(\mathbf{x}) = l)$ and $\mathbb{P}(\hat{\Gamma}_{-j_\tau}(\mathbf{x}) = l)$, which are the probability mass functions of Poisson-binomial random variables $\hat{\Gamma}(\mathbf{x})$ and $\hat{\Gamma}_{-j_\tau}(\mathbf{x})$, respectively. As indicated in Hong (2013), they can be efficiently evaluated by a fast Fourier transformation (FFT). Based on the numerical results in Hong (2013), the computing time for FFT evaluation with $d \leq 500$ is generally negligible (less than ten milliseconds). Moreover, it is worth noting that our algorithm in (9) needs not store the entire auxiliary matrix $(\boldsymbol{\omega}_1(\mathbf{x}), \dots, \boldsymbol{\omega}_d(\mathbf{x}))$, since the τ -th row $\boldsymbol{\omega}_\tau$ can be computed from the previous row $\boldsymbol{\omega}_{\tau-1}$. Hence, only $O(d)$ storage is required in (9). The detailed algorithm is summarized in Algorithm 1 with `approx=False`.

2.3.2 APPROXIMATION ALGORITHMS FOR HIGH-DIMENSIONAL SEGMENTATION

For high-dimensional segmentation, especially for image segmentation, it is challenging to solve (6) by a grid searching over $\tau \in \{0, \dots, d\}$. To address this issue, we use shrinkage and approximation techniques to reduce the computational complexity of (6). First, Lemma 2 is developed to shrink the searching range of τ .

Lemma 2 (shrinkage) *If $\sum_{s=1}^{\tau} \hat{q}_{j_s}(\mathbf{x}) \geq (\tau + \gamma + d) \hat{q}_{j_{\tau+1}}(\mathbf{x})$, then $\bar{\pi}_{\tau}(\mathbf{x}) \geq \bar{\pi}_{\tau'}(\mathbf{x})$ for all $\tau' > \tau$.*

Lemma 2 can be viewed as an early stopping of the grid searching. Accordingly, we can shrink the grid search in (6) from $\{0, \dots, d\}$ to $\{0, \dots, d_0(\mathbf{x})\}$, which significantly reduces the computational complexity. Specifically,

$$\hat{\tau}(\mathbf{x}) = \underset{\tau \in \{0, \dots, d_0(\mathbf{x})\}}{\operatorname{argmax}} \bar{\pi}_{\tau}(\mathbf{x}); \quad d_0(\mathbf{x}) = \min \left\{ \tau = 1, \dots, d : \sum_{s=1}^{\tau} \hat{q}_{j_s}(\mathbf{x}) / \hat{q}_{j_{\tau+1}}(\mathbf{x}) \geq \tau + \gamma + d \right\}. \quad (10)$$

In many applications, $d_0(\mathbf{x})$ is upper bounded by a small integer, that is, $d_0(\mathbf{x}) < d_U \ll d$, called the *well-separated segmentation*. For example, there exists a small number of features/pixels whose probabilities (close to 1) are much larger than the others.

Truncated refined normal approximation (T-RNA). Note that the cumulative distribution function (CDF), and thus the probability mass function, of a Poisson-binomial random variable can be efficiently evaluated by a refined normal approximation when the dimension is large (Hong, 2013; Neammanee, 2005). For instance,

$$\begin{aligned} \mathbb{P}(\hat{\Gamma}(\mathbf{x}) \leq l) &\leftarrow \tilde{\mathbb{P}}(\hat{\Gamma}(\mathbf{x}) \leq l) := \Psi(\hat{\sigma}^{-1}(l + 1/2 - \hat{\mu}(\mathbf{x}))), \\ \mathbb{P}(\hat{\Gamma}_{-j}(\mathbf{x}) \leq l) &\leftarrow \tilde{\mathbb{P}}(\hat{\Gamma}_{-j}(\mathbf{x}) \leq l) := \Psi_{-j}(\hat{\sigma}_{-j}^{-1}(l + 1/2 - \hat{\mu}_{-j}(\mathbf{x}))), \end{aligned} \quad (11)$$

where $\Psi(u) = \Phi(u) + \hat{\eta}(\mathbf{x})(1 - u^2)\phi(u)/6$ and $\Psi_{-j}(u) = \Phi(u) + \hat{\eta}_{-j}(\mathbf{x})(1 - u^2)\phi(u)/6$ are two skew-corrected refined normal CDFs, $\Phi(\cdot)$ is the CDF of the standard normal distribution, and $(\hat{\mu}(\mathbf{x}), \hat{\mu}_{-j}(\mathbf{x}))$, $(\hat{\sigma}^2(\mathbf{x}), \hat{\sigma}_{-j}^2(\mathbf{x}))$, $(\hat{\eta}(\mathbf{x}), \hat{\eta}_{-j}(\mathbf{x}))$ are mean, variance and skewness of the Poisson-binomial random variables $\hat{\Gamma}(\mathbf{x})$ and $\hat{\Gamma}_{-j}(\mathbf{x})$, respectively. See the definitions of variance and skewness of the Poisson-binomial distribution in Appendix B.3.

On this ground, it is unnecessary to compute all $\mathbb{P}(\hat{\Gamma}_{-j}(\mathbf{x}) = l)$ and $\mathbb{P}(\hat{\Gamma}(\mathbf{x}) = l)$ for $l = 1, \dots, d$, since they are negligibly close to zero when l is too small or too large. In other words, many $\mathbb{P}(\hat{\Gamma}_{-j}(\mathbf{x}) = l)$ and $\mathbb{P}(\hat{\Gamma}(\mathbf{x}) = l)$ can be ignored when evaluating $\bar{\omega}_{\tau}$ and \bar{v}_{τ} . Therefore, according to the refined normal approximation in (11), $\bar{\omega}_{\tau}$ and \bar{v}_{τ} can be approximated by only taking a partial sum over a subset of $l = 0, \dots, d$:

$$\begin{aligned} \tilde{\omega}_{\tau}(\mathbf{x}) &= \sum_{l \in \mathcal{L}(\varepsilon)} \frac{2\tilde{\omega}_{\tau,l}(\mathbf{x})}{\tau + l + \gamma + 1}, \quad \tilde{v}_{\tau}(\mathbf{x}) = \sum_{l \in \mathcal{L}(\varepsilon)} \frac{\gamma \tilde{\mathbb{P}}(\hat{\Gamma}(\mathbf{x}) = l)}{\tau + l + \gamma}, \quad \tilde{\omega}_{\tau,l}(\mathbf{x}) = \sum_{s=1}^{\tau} \hat{q}_{j_s}(\mathbf{x}) \tilde{\mathbb{P}}(\hat{\Gamma}_{-j_s}(\mathbf{x}) = l), \\ \mathcal{L}(\varepsilon) &= \left\{ \lfloor \hat{\sigma}(\mathbf{x})\Psi^{-1}(\varepsilon) + \hat{\mu}(\mathbf{x}) - \frac{3}{2} \rfloor, \dots, \lfloor \hat{\sigma}(\mathbf{x})\Psi^{-1}(1 - \varepsilon) + \hat{\mu}(\mathbf{x}) - \frac{1}{2} \rfloor \right\} \cap \{0, \dots, d\}, \end{aligned} \quad (12)$$

where $\tilde{\mathbb{P}}(\hat{\Gamma}(\mathbf{x}) = l) := \tilde{\mathbb{P}}(\hat{\Gamma}(\mathbf{x}) \leq l) - \tilde{\mathbb{P}}(\hat{\Gamma}(\mathbf{x}) \leq l - 1)$, $\tilde{\mathbb{P}}(\hat{\Gamma}_{-j}(\mathbf{x}) = l) := \tilde{\mathbb{P}}(\hat{\Gamma}_{-j}(\mathbf{x}) \leq l) - \tilde{\mathbb{P}}(\hat{\Gamma}_{-j}(\mathbf{x}) \leq l - 1)$, $\Psi^{-1}(\cdot)$ is the quantile function of the refined normal distribution, and ε is a custom tolerance error. The detailed algorithm is summarized in Algorithm 1 with `approx='T-RNA'`. Moreover, the following lemma quantifies the approximation error of the proposed approximate algorithm.

Lemma 3 For $(\bar{\omega}_\tau, \bar{v}_\tau)$ and $(\tilde{\omega}_\tau, \tilde{v}_\tau)$ defined in (8) and (12) respectively, if $\hat{\sigma}^2(\mathbf{x}) \geq 25$, then for any $\tau \in \{0, \dots, d\}$, we have

$$\begin{aligned} |\tilde{\omega}_\tau - \bar{\omega}_\tau| &\leq \frac{4\tau}{\tau + \gamma + 1} \left(\varepsilon + \frac{C_0}{\hat{\sigma}^2(\mathbf{x})} \right) + \frac{C_0 \min(\hat{\mu}(\mathbf{x}), \tau)}{\hat{\sigma}^2(\mathbf{x}) - 1/4} \left(\log(1+d) + 1 \right), \\ |\tilde{v}_\tau - \bar{v}_\tau| &\leq \frac{2\gamma}{\tau + \gamma} \left(\varepsilon + \frac{C_0}{\hat{\sigma}^2(\mathbf{x})} \right) + \frac{C_0 \gamma}{\hat{\sigma}^2(\mathbf{x})} \left(\log(1+d) + 1 \right), \end{aligned}$$

where $C_0 = 0.1618$ if $\hat{\sigma}^2(\mathbf{x}) \geq 100$, and $C_0 = 0.3056$ if $\hat{\sigma}^2(\mathbf{x}) \geq 25$. Moreover, when $d \rightarrow \infty$, we have

$$|\tilde{\pi}_\tau - \bar{\pi}_\tau| \leq \left(\frac{4\tau}{\tau + \gamma + 1} + \frac{2\gamma}{\tau + \gamma} \right) \varepsilon + O\left(\frac{\min(\hat{\mu}(\mathbf{x}), \tau) \log(d)}{\hat{\sigma}^2(\mathbf{x})} \right).$$

Here we define $0/0 := 0$ for $\gamma/(\tau + \gamma)$ when $\tau = \gamma = 0$.

Note that $\hat{\sigma}^2(\mathbf{x}) = \sum_{j=1}^d \hat{q}_j(\mathbf{x})(1 - \hat{q}_j(\mathbf{x}))$ is the variance of $\hat{\Gamma}(\mathbf{x})$, which often tends to infinity as $d \rightarrow \infty$. In image segmentation, the dimension d varies from 1024 (32x32) to 262144 (512x512). Therefore, the error bound is practical for high-dimensional segmentation. Moreover, ε is the tolerance error to balance the approximation error and computation complexity. For instance, when ε becomes smaller, the approximation error decreases, the computation complexity increases with an enlarged $\mathcal{L}(\varepsilon)$. Typically, $\Psi^{-1}(1 - \varepsilon) - \Psi^{-1}(\varepsilon) \leq 7.438$ when $\varepsilon = 1e-4$. Based on the approximation formula (12), the worst-case computational complexity is reduced to $O(d\hat{\sigma}(\mathbf{x}))$ for general segmentation and $O(\hat{\sigma}(\mathbf{x}))$ for *well-separated segmentation* ($d_0(\mathbf{x}) \leq d_U$). The computational complexity is summarized in Table 1 (based on $\varepsilon = 1e-4$).

Although T-RNA significantly reduces the computational complexity, yet this algorithm uses recursive updates, making it difficult in parallel computing on GPUs. For example, due to the memory issues, recursive function calls are restricted in the CUDA (Compute Unified Device Architecture) kernels (Nickolls et al., 2008). Next, we propose the blind approximation algorithm to exploit GPU-computing for the proposed *RankDice*.

Blind approximation (BA). In high-dimensional segmentation, the difference in distributions between $\hat{\Gamma}(\mathbf{x})$ and $\hat{\Gamma}_{-j}(\mathbf{x})$ is negligible. Inspired by this fact, we propose a novel approximation algorithm, namely the blind approximation, to simultaneously evaluate the score functions with a small error tolerance. Specifically, based on the refined normal approximation, we further simplify the evaluation formulas by replacing $\tilde{\mathbb{P}}(\hat{\Gamma}_{-j_s}(\mathbf{x}) = l)$ as $\tilde{\mathbb{P}}(\hat{\Gamma}(\mathbf{x}) = l)$:

$$\tilde{\omega}_\tau^b(\mathbf{x}) = 2 \sum_{s=1}^{\tau} \hat{q}_{j_s}(\mathbf{x}) \sum_{l \in \mathcal{L}(\varepsilon)} \frac{\tilde{\mathbb{P}}(\hat{\Gamma}(\mathbf{x}) = l)}{\tau + l + \gamma + 1}, \quad \tilde{v}_\tau^b(\mathbf{x}) = \tilde{v}_\tau(\mathbf{x}) = \sum_{l \in \mathcal{L}(\varepsilon)} \frac{\gamma \tilde{\mathbb{P}}(\hat{\Gamma}(\mathbf{x}) = l)}{\tau + l + \gamma},$$

where $\mathcal{L}(\varepsilon) = \{l_L, \dots, l_U\}$ is defined in (12). Then, for any $1 \leq d_0 \leq d$, $\tilde{\omega}_{1:T}^b = (\tilde{\omega}_1^b, \dots, \tilde{\omega}_T^b)^\top$ and $\tilde{v}_{1:T}^b = (\tilde{v}_1^b, \dots, \tilde{v}_T^b)^\top$ can be simultaneously computed over $\tau = 0, \dots, d_0$ based on cross-correlation (flipped convolution (Tahmasebi et al., 2012)):

$$\begin{aligned} \tilde{\omega}_{1:d_0}^b &= 2\hat{\mathbf{s}}_{1:d_0}(\mathbf{x}) \circ \left((\tilde{\mathbb{P}}(\hat{\Gamma}(\mathbf{x}) = l_L), \dots, \tilde{\mathbb{P}}(\hat{\Gamma}(\mathbf{x}) = l_U))^\top \star \left(\frac{1}{l_L + \gamma + 1}, \dots, \frac{1}{l_U + \gamma + d_0 + 1} \right) \right), \\ \tilde{v}_{1:d_0}^b &= \gamma \left((\tilde{\mathbb{P}}(\hat{\Gamma}(\mathbf{x}) = l_L), \dots, \tilde{\mathbb{P}}(\hat{\Gamma}(\mathbf{x}) = l_U))^\top \star \left(\frac{1}{l_L + \gamma}, \dots, \frac{1}{l_U + \gamma + d_0} \right) \right), \end{aligned} \quad (13)$$

Algorithm 1: Computing schemes for the proposed RankDice framework.

Input : Training set: $(\mathbf{x}_i, \mathbf{y}_i)_{i=1}^n$; A new testing instance: \mathbf{x} ; Approx method: approx

Output: The predicted segmentation for the testing instance $\hat{\boldsymbol{\delta}}(\mathbf{x})$

- 1 **Conditional prob est.** Estimate conditional prob $\hat{\mathbf{q}}$ via (5) based on training set $(\mathbf{x}_i, \mathbf{y}_i)_{i=1}^n$;
- 2 **Ranking.** Rank estimated conditional probabilities for \mathbf{x} , and denote the indices in sorted order as j_1, \dots, j_d , that is, $\hat{q}_{j_1}(\mathbf{x}) \geq \hat{q}_{j_2}(\mathbf{x}) \geq \dots \geq \hat{q}_{j_d}(\mathbf{x})$;
- 3 **Volume estimation.**
- 4 Compute and store the cumulative sum of sorted estimated probabilities $\hat{\mathbf{s}}(\mathbf{x})$;
- 5 Compute $d_0(\mathbf{x})$ based on $\hat{\mathbf{s}}(\mathbf{x})$ via (10);
- 6 **if** approx is None **then**
- 7 | $\mathcal{L} = \{0, \dots, d\}$;
- 8 **else**
- 9 | $\mathcal{L} = \mathcal{L}(\varepsilon) = \{l_L, \dots, l_U\}$ based on (12);
- 10 **end**
- 11 Compute and store $\mathbb{P}(\hat{\Gamma}(\mathbf{x}) = l)$ for $l \in \mathcal{L}$;
- 12 **if** approx is BA **then**
- 13 | Compute and store $\tilde{\omega}_{1:d_0(\mathbf{x})}^b$ and $\tilde{\nu}_{1:d_0(\mathbf{x})}^b$ based on (13);
- 14 **else**
- 15 | Initialize $\omega_{old} = \mathbf{0}$;
- 16 | **for** $\tau = 1, \dots, d_0(\mathbf{x})$ **do**
- 17 | | Update ω_{new} as
- $\omega_{new,l} \leftarrow \omega_{old,l} + \hat{q}_{j_\tau}(\mathbf{x}) \mathbb{P}(\hat{\Gamma}_{-j_\tau}(\mathbf{x}) = l)$, for $l \in \mathcal{L}$, $\omega_{old} \leftarrow \omega_{new}$,
- where $\hat{\Gamma}_{-j}(\mathbf{x})$ is Poisson binomial r.v. with the success probabilities $\hat{\mathbf{q}}_{-j}(\mathbf{x})$;
- 18 | | Compute and store $\bar{\pi}_\tau = \bar{\omega}_\tau + \bar{\nu}_\tau = \sum_{l \in \mathcal{L}} \frac{1}{\tau+l+1} \omega_{new,l} + \sum_{l \in \mathcal{L}} \frac{\gamma}{\tau+l+\gamma} \mathbb{P}(\hat{\Gamma}(\mathbf{x}) = l)$;
- 19 | **end**
- 20 **end**
- 21 Estimate $\hat{\tau}(\mathbf{x}) = \operatorname{argmax}_{\tau=0, \dots, d_0(\mathbf{x})} \bar{\pi}_\tau$ via (8);
- 22 **Prediction.** The predicted segmentation is provided as:

$$\hat{\delta}_j(\mathbf{x}) = 1, \text{ if } j \in \{j_1, \dots, j_{\hat{\tau}(\mathbf{x})}\}; \quad \hat{\delta}_j(\mathbf{x}) = 0, \text{ otherwise.}$$

return The predicted segmentation $\hat{\boldsymbol{\delta}}(\mathbf{x}) = (\hat{\delta}_1(\mathbf{x}), \dots, \hat{\delta}_d(\mathbf{x}))^\top$.

where $\widehat{\mathbf{s}}(\mathbf{x}) = (\widehat{s}_1(\mathbf{x}), \dots, \widehat{s}_d(\mathbf{x}))^\top$ and $\widehat{s}_K(\mathbf{x}) = \sum_{k=1}^K \widehat{q}_{j_k}(\mathbf{x})$ is the cumulative sum of sorted estimated probabilities, \circ is element-wise product of two vectors, and \star is the cross-correlation operator (flipped convolution) of two vectors (Tahmasebi et al., 2012). Notably, the cross-correlation can be efficiently implemented by a fast Fourier transform (Bracewell and Bracewell, 1986) with time complexity $O((d_0 + \widehat{\sigma}(\mathbf{x})) \log(d_0 + \widehat{\sigma}(\mathbf{x})))$. Besides, the overall time complexity with CUDA implementation on GPUs can be further reduced by parallel computing. The detailed algorithm is summarized in Algorithm 1 with `approx='BA'`. Next, Lemma 4 shows the approximation error of the proposed blind approximation algorithm.

Lemma 4 For $(\bar{\omega}_\tau, \bar{v}_\tau)$ and $(\tilde{\omega}_\tau^b, \tilde{v}_\tau^b)$ defined in (8) and (13) respectively, if $\widehat{\sigma}^2(\mathbf{x}) \geq 25$, then for any $\tau \in \{0, \dots, d\}$, and any $\gamma \geq 0$, we have

$$\begin{aligned} |\tilde{\omega}_\tau^b - \bar{\omega}_\tau| &\leq \frac{4\tau}{\tau + \gamma + 1} \left(\varepsilon + \frac{C_0}{\widehat{\sigma}^2(\mathbf{x})} \right) + \frac{C_0 \min(\widehat{\mu}(\mathbf{x}), \tau)}{\widehat{\sigma}^2(\mathbf{x}) - 1/4} \left(\log(1 + d) + 1 \right) \\ &\quad + \frac{1}{4\sqrt{2\pi}} \left(\frac{1/(2\sqrt{e})}{\widehat{\sigma}^2(\mathbf{x}) - 1/4} + \frac{4}{\sqrt{\widehat{\sigma}^2(\mathbf{x}) - 1/4}} + \frac{4\widehat{m}_3(\mathbf{x})}{(\widehat{\sigma}^2(\mathbf{x}) - 1/4)^{3/2}} \right) \left(\log(1 + d) + 1 \right), \end{aligned}$$

where $\widehat{m}_3(\mathbf{x}) = \sum_{j=1}^d \widehat{q}_j(\mathbf{x})(1 - \widehat{q}_j(\mathbf{x}))(1 - 2\widehat{q}_j(\mathbf{x}))$, $C_0 = 0.1618$ if $\widehat{\sigma}^2(\mathbf{x}) \geq 100$, and $C_0 = 0.3056$ if $\widehat{\sigma}^2(\mathbf{x}) \geq 25$. Specifically, when $d \rightarrow \infty$, we have

$$|\tilde{\pi}_\tau - \bar{\pi}_\tau| \leq \left(\frac{4\tau}{\tau + \gamma + 1} + \frac{2\gamma}{\tau + \gamma} \right) \varepsilon + O\left(\left(\frac{\min(\widehat{\mu}(\mathbf{x}), \tau)}{\widehat{\sigma}^2(\mathbf{x})} + \frac{1}{\widehat{\sigma}(\mathbf{x})} \right) \log(d) \right).$$

In contrast to the truncated refined normal approximation, the blind approximation algorithm significantly reduces the time complexity and enables GPU parallel execution. On the other hand, the blind approximation leads to an additional $\widehat{\sigma}^{-1}(\mathbf{x})$ in Lemma 4 compared with that of T-RNA in Lemma 3, yet the error bound is still acceptable in practice.

Taken together, we summarize the foregoing computational schemes in Algorithm 1, and their inference (after obtaining conditional probabilities) computational complexity (worst-case) is indicated in Table 1. For the threshold-based framework, thresholding the estimated probabilities takes $O(d)$ time complexity. For the proposed method, Step 2 takes $O(d \log(d))$ based on the merge sort (Ajtai et al., 1983), and Step 3 takes $O(d_0(\mathbf{x})\widehat{\sigma}(\mathbf{x}))$ based on T-RNA in (10) and (11), and takes $O(d_0(\mathbf{x}) \log(d_0(\mathbf{x})))$ based on BA in (13).

3. mDice-segmentation and mRankDice

In this section, we discuss the extension of the proposed *RankDice* framework to segmentation with multiclass/multilabel outcomes evaluated by the mDice metric. Overall, multiclass/multilabel segmentation differs from Dice-segmentation in a number of important aspects. First, a new evaluation metric called mDice is introduced. Second, multiclass/multilabel outcomes provide two different ways of probabilistic modeling. Third, whether (or not) to allow for overlapping segmentation results among different classes leads to different problem setups. These aspects will be discussed in detail in the following subsections.

3.1 The mDice metric

For multiclass/multilabel segmentation, $(\mathbf{X}, \mathbf{Y}_1, \dots, \mathbf{Y}_K)$ is available, where $\mathbf{X} \in \mathbb{R}^d$ represents a feature vector, K is the total number of classes of interest, $\mathbf{Y}_k \in \{0, 1\}^d$ is the true feature-wise

SEG framework	Time	Time (well-separated)	Memory
Threshold-based SEG	$O(d)$	$O(d)$	$O(d)$
RankDice (our)	$O(d \log(d) + dd_0(\mathbf{x}))$	$O(d \log(d))$	$O(d)$
RankDice-RNA (our)	$O(d \log(d) + \widehat{\sigma}(\mathbf{x})d_0(\mathbf{x}))$	$O(d \log(d))$	$O(d)$
RankDice-BA (our)	$O(d_0(\mathbf{x}) \log(d_0(\mathbf{x})))$	$O(d \log(d))$	$O(d)$

Table 1: Inference (prediction) computational complexity for the segmentation frameworks. Here “Time” denotes the time complexity, “Memory” denotes the amount of storage needed including probability outcomes, “Time (well-separated)” denotes the time complexity on *well-separated segmentation* ($d_0(\mathbf{x}) \leq d_U$), and $d_0(\mathbf{x}) \leq d$ is the reduced dimension defined in (10), $\widehat{\sigma}(\mathbf{x})$ is the standard deviation of $\widehat{\Gamma}(\mathbf{x})$ with at most an order of $O(\sqrt{d})$. Note that the time complexity of RankDice-BA can be further reduced by GPU implementation. See more detailed discussion in Section 2.3.

segmentation label for the k -th class, where $Y_{jk} = 1$ indicates that the j -th feature X_j is segmented under the k -th class, and $I(\mathbf{Y}_{\cdot k}) = \{j : Y_{jk} = 1; \text{ for } j = 1, \dots, d\}$ is the class-specific index set for all segmented features.

On this ground, a class-specific segmentation operator $\Delta_k : \mathbb{R}^d \rightarrow \{0, 1\}^d$ ($k = 1, \dots, K$) is introduced, where $\Delta_{jk}(\mathbf{x}) \in \{0, 1\}$ is the predicted segmentation for the class k of the j -th feature, and $I(\Delta_k(\mathbf{X})) = \{j : \Delta_{jk}(\mathbf{X}) = 1; \text{ for } j = 1, \dots, d\}$ is the class-specific index set of features for the predicted segmentation. Then, given a segmentation operator $\Delta = (\Delta_1, \dots, \Delta_K)$, the multi-Dice (mDice) metric is defined as:

$$\begin{aligned} \text{mDice}_{\gamma}(\Delta) &= \sum_{k=1}^K \alpha_k \text{Dice}_{\gamma, k}(\Delta_k) \\ &= \sum_{k=1}^K \alpha_k \mathbb{E} \left(\frac{2|I(\mathbf{Y}_{\cdot k}) \cap I(\Delta_k(\mathbf{X}))| + \gamma}{|I(\mathbf{Y}_{\cdot k})| + |I(\Delta_k(\mathbf{X}))| + \gamma} \right) = \sum_{k=1}^K \alpha_k \mathbb{E} \left(\frac{2\mathbf{Y}_{\cdot k}^\top \Delta_k(\mathbf{X}) + \gamma}{\|\mathbf{Y}_{\cdot k}\|_1 + \|\Delta_k(\mathbf{X})\|_1 + \gamma} \right), \end{aligned} \quad (14)$$

where $\text{Dice}_{\gamma, k}(\cdot)$ is the Dice metric under the k -th class, $\boldsymbol{\alpha} = (\alpha_1, \dots, \alpha_K)^\top \geq \mathbf{0}_K$ is a weight vector for classes with $\|\boldsymbol{\alpha}\|_1 = 1$. For example, $\alpha_k = 1/K$ yields that each class has the same contribution to segmentation performance. More generally, $\boldsymbol{\alpha} \geq \mathbf{0}_K$ can be a custom weight vector indicating the relative importance of segmentation classes. In practice, given a new instance (\mathbf{x}, \mathbf{y}) , the weight is an average over classes excluding those are not present and not predicted, that is,

$$\alpha_k = 0, \text{ if } \|\mathbf{y}_{\cdot k}\|_1 = \|\Delta_k(\mathbf{x})\|_1 = 0; \quad \alpha_k = \frac{1}{\sum_{k=1}^K \mathbf{1}(\|\mathbf{y}_{\cdot k}\|_1 + \|\Delta_k(\mathbf{x})\|_1 > 0)}, \text{ otherwise.} \quad (15)$$

Following our convention, we shall call multiclass/multilabel segmentation with respect to the mDice metric as “mDice-segmentation”. As indicated in Figure 2, unlike Dice-segmentation, mDice-segmentation provides more flexibility in probabilistic modeling (multiclass or multilabel) and the decision-making in prediction (taking argmax or thresholding at 0.5), resulting in different operating losses and the construction of predictive functions.

3.2 Multilabel/multiclass outcomes

In this section, we describe two probabilistic models (multilabel or multiclass) of $\mathbf{Y}_j|\mathbf{X}$, where $\mathbf{Y}_j = (Y_{j1}, \dots, Y_{jK})^\top$ is the true label for the j -th feature.

For multilabel modeling, we assume each feature could be assigned to multiple classes, that is, $\|\mathbf{Y}_j\|_1 \in \{0, \dots, K\}$, for $j = 1, \dots, d$. As a result, the index sets of segmented features may overlap among classes. In this case, we formulate and estimate $q_{jk}(\mathbf{x})$ under a multilabel probabilistic model. For example, for deep learning models, we use the sigmoid function as the output layer activation function of a neural network with the *binary cross-entropy* loss.

For multiclass modeling, each feature is assigned to one and only one class, that is, $\|\mathbf{Y}_j\|_1 = 1$ for $j = 1, \dots, d$. An instance is the panoptic annotation in image segmentation. In this case, we formulate and estimate $\mathbf{q}_j(\mathbf{x}) = (q_{j1}(\mathbf{x}), \dots, q_{jK}(\mathbf{x}))^\top$ under a multiclass model with additional sum-to-one constraints $\|\mathbf{q}_j(\mathbf{x})\|_1 = 1$ for $j = 1, \dots, d$ and $\mathbf{x} \in \mathbb{R}^d$. Specifically, for deep learning models, we use the softmax function as the output layer activation function of a neural network, which automatically enforces the sum-to-one constraints. Correspondingly, a multiclass loss is used as an operating loss, including the *multiclass cross-entropy*. Note that the Dice-approximating losses, such as the soft-Dice loss, can be adopted into the multilabel/multiclass modeling.

In literature, once the estimation is done, the predicted segmentation is produced by taking *argmax* or *thresholding* at 0.5 on the estimated probabilities. Indeed, *argmax* and *thresholding* are inspired by the decision-making in multiclass and multilabel classification, respectively. In segmentation, it is possible to attempt ad-hoc combinations, such as multiclass modeling + *thresholding*, and multilabel modeling + *argmax*. The major purpose of *argmax* is to provide *non-overlapping* prediction (e.g., the panoptic prediction in image segmentation). We discuss overlapping/non-overlapping segmentation in the next section.

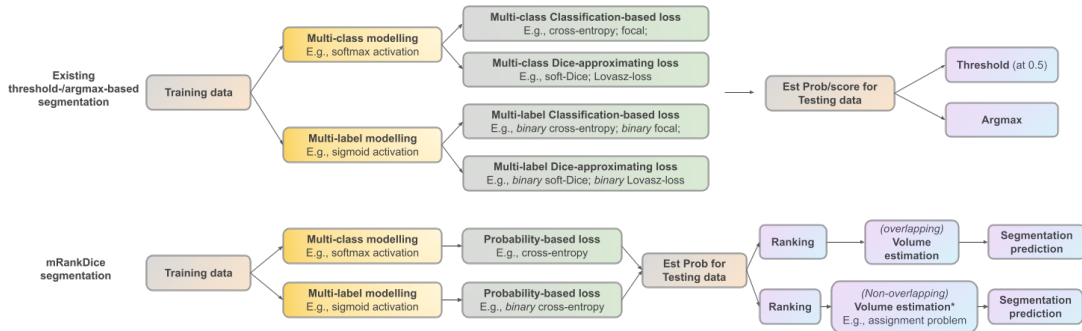


Figure 2: The existing and the proposed frameworks under multiclass/multilabel modeling. The upper panel is *threshold-/argmax-based segmentation*, and the lower panel is the proposed *mRankDice* framework.

3.3 Overlapping or non-overlapping mDice-segmentation

Specifically, whether (or not) to allow for overlapping results among distinct classes leads to different decision-making procedures, namely overlapping/non-overlapping mDice-segmentation:

$$\begin{aligned} \text{(Overlapping)} \quad \underset{\Delta}{\operatorname{argmax}} \quad \text{mDice}_{\gamma}(\Delta), \quad \text{(Non-overlapping)} \quad \underset{\Delta}{\operatorname{argmax}} \quad \text{mDice}_{\gamma}(\Delta), \quad \sum_{k=1}^K \Delta_k(\cdot) = \mathbf{1}_d. \end{aligned} \quad (16)$$

In the overlapping setting, there is no restriction on a segmentation operator, thus the predicted segmentation for different classes may overlap. On the other hand, the overlapping is ruled out in non-overlapping formulation due the additional sum-to-one constraint. Lemma 5 presents the Bayes rule for overlapping segmentation, yielding that mDice-segmentation is reduced class-specific Dice-segmentation subproblems if overlapping is allowed.

Lemma 5 (The Bayes rule for overlapping mDice-segmentation) *An overlapping (allowing) segmentation operator Δ^* is a global maximizer of $\text{mDice}_{\gamma}(\Delta)$ if and only if Δ_k^* is the Bayes rule (global maximizer) of $\text{Dice}_{\gamma,k}(\Delta_k)$ on $(\mathbf{X}, \mathbf{Y}_k)$ for all $k \in \{1 \leq k \leq K : \alpha_k > 0\}$.*

Therefore, it suffices to consider Dice-segmentation of each class separately in overlapping mDice-segmentation, and the proposed *RankDice* is readily extended to *mRankDice*; see Section 3.4.

Next, we investigate the Bayes rule for non-overlapping mDice-segmentation. To proceed, we denote Δ^* as the Bayes rule (global maximizer) of non-overlapping mDice-segmentation in (16), and $\boldsymbol{\tau}^*(\cdot)$ as the volume function of the Bayes segmentation rule: $\boldsymbol{\tau}^*(\mathbf{x}) = (\tau_1^*(\mathbf{x}), \dots, \tau_K^*(\mathbf{x}))^\top = (\|\Delta_1^*(\mathbf{x})\|_1, \dots, \|\Delta_K^*(\mathbf{x})\|_1)^\top$.

Lemma 6 *Suppose $\boldsymbol{\tau}^*(\cdot)$ is pre-known, then solving the Bayes rule for non-overlapping mDice-segmentation in (16) is equivalent to an assignment problem.*

As indicated in Lemma 6, even when the optimal volume function is pre-given, solving the Bayes rule for non-overlapping segmentation is nontrivial. For example, the most successful assignment algorithms, including the Hungarian method (Kuhn, 1955; Edmonds and Karp, 1972; Tomizawa, 1971) and its variants Jonker-Volgenant algorithm (Crouse, 2016), generally achieves an $O(d^3)$ running time complexity in our content, which is time-consuming for high-dimensional segmentation. In sharp contrast, for the overlapping case, when $\boldsymbol{\tau}^*(\mathbf{x})$ is given, the Bayes rule is simply ranking all the conditional probabilities with $O(d \log(d))$. Moreover, when $\boldsymbol{\tau}^*(\mathbf{x})$ is unknown, the optimization for non-overlapping segmentation becomes a nonlinear integer optimization which is NP-hard in general (Murty and Kabadi, 1985; D’Ambrosio et al., 2020). Therefore, a fast $O(d \log(d))$ greedy approximation algorithm is more feasible in practical implementation. We leave pursuing this topic as future work.

Next, we summarize the proposed *mRankDice* framework under three scenarios.

3.4 mRankDice

In this section, we present the proposed *mRankDice* framework for mDice-segmentation. Before we proceed, we highlight the different roles of multiclass/multilabel modeling and the overlapping/non-overlapping constraint. Multiclass/multilabel modeling determines the probabilistic models (say

the softmax or the sigmoid activation in a neural network) and an operating loss in probability estimation (say the cross-entropy or the binary cross-entropy). Meanwhile, the overlapping/non-overlapping constraint affects the segmentation prediction after the probabilities are estimated.

Therefore, we consider following segmentation three cases: “multilabel + overlapping”, “multiclass + overlapping”, and “multilabel/multiclass + non-overlapping”.

mRankDice (multilabel + overlapping segmentation) is a straightforward extension of *RankDice* in Dice-segmentation (inspired by Lemma 5). Given a training dataset $(\mathbf{x}_i, \mathbf{y}_{i,1:d,1}, \dots, \mathbf{y}_{i,1:d,K})_{i=1}^n$, with the same manner, the conditional probability function is estimated under a multilabel logistic regression (the binary cross-entropy loss):

$$\hat{\mathbf{Q}}(\mathbf{x}) = \underset{\mathbf{Q} \in \mathcal{Q}}{\operatorname{argmin}} \sum_{i=1}^n \sum_{j=1}^d \sum_{k=1}^K \left(y_{ijk} \log(q_{jk}(\mathbf{x}_i)) + (1 - y_{ijk}) \log(1 - q_{jk}(\mathbf{x}_i)) \right) + \lambda \|\mathbf{Q}\|^2, \quad (17)$$

where $\mathbf{Q} = (q_{jk}) : \mathbb{R}^d \rightarrow [0, 1]^{d \times K}$ is a matrix function, and $q_{jk}(\mathbf{x})$ is a candidate estimator of $p_{jk}(\mathbf{x})$. Then, given a new instance \mathbf{x} , the class-specific segmentation $\hat{\Delta}_k(\mathbf{x})$ is generated based on **Steps 2-3** in Section 2.2 with the estimated conditional probabilities $\hat{\mathbf{Q}}_k(\mathbf{x})$ (the k -th column of $\hat{\mathbf{Q}}(\mathbf{x})$). We summarize the foregoing computational scheme in Algorithm 2.

mRankDice (multiclass + overlapping segmentation) yields a different probability estimation procedure, where the conditional probability function is estimated under a multiclass logistic regression (the multiclass cross-entropy loss):

$$\hat{\mathbf{Q}}(\mathbf{x}) = \underset{\mathbf{Q} \in \mathcal{Q}}{\operatorname{argmin}} \sum_{i=1}^n \sum_{j=1}^d \sum_{k=1}^K y_{ijk} \log(q_{jk}(\mathbf{x}_i)) + \lambda \|\mathbf{Q}\|^2, \quad \text{s.t.} \quad \sum_{k=1}^K q_{jk}(\cdot) = 1; \text{ for } j = 1, \dots, d, \quad (18)$$

where $\mathbf{Q} = (q_{jk}) : \mathbb{R}^d \rightarrow [0, 1]^{d \times K}$ is a matrix function, and $\mathbf{q}_j(\mathbf{x})$ is a candidate estimator of $\mathbf{p}_j(\mathbf{x})$. Although the probability estimation (18) differs from (17), the downstream ranking and volume estimation remain the same according to Lemma 5. We also summarize the foregoing computational scheme in Algorithm 2.

Algorithm 2: mRankDice for overlapping mDice-segmentation.

Input : Training set: $(\mathbf{x}_i, \mathbf{y}_{i,1:d,1}, \dots, \mathbf{y}_{i,1:d,K})_{i=1}^n$; A new testing instance: \mathbf{x}
Output: The predicted segmentation for the testing instance $\hat{\Delta}(\mathbf{x})$

- 1 **if** *multilabel outcome* **then**
- 2 **Multilabel Prob Est.** Estimate the prob function $\hat{\mathbf{Q}}$ via (17);
- 3 **end**
- 4 **if** *multiclass outcome* **then**
- 5 **Multiclass Prob Est.** Estimate the prob function $\hat{\mathbf{Q}}$ via (18);
- 6 **end**
- 7 **for** $k = 1, \dots, K$ **do**
- 8 **Class-specific RankDice.** Obtain $\hat{\Delta}_k(\mathbf{x})$ from Lines 2-22 in Algorithm 1 based on the estimated prob $\hat{\mathbf{Q}}_k(\mathbf{x})$.
- 9 **end**
- 10 **return** *The predicted segmentation* $\hat{\Delta}(\mathbf{x}) = (\hat{\Delta}_1(\mathbf{x}), \dots, \hat{\Delta}_K(\mathbf{x}))$

mRankDice (multiclass/multilabel + non-overlapping segmentation) is a quite difficult scenario for developing *mRankDice* from *RankDice* in Dice-segmentation. As indicated in Lemma 6, searching for an optimal non-overlapping mDice-segmentation operator is NP-hard in general. We leave pursuing this topic as future work.

4. Theory

In this section, we establish a theoretical foundation of segmentation, including the concept of Dice-calibration, the excess risk of the Dice metric, and the rate of convergence with respect to the excess risk of the proposed *RankDice* framework. For illustration, we focus on Dice-segmentation, and the results can be extended to overlapping mDice-segmentation, and *RankIoU* in terms of the IoU metric.

4.1 Dice-calibrated segmentation

In Theorem 1, the Bayes rule of Dice-segmentation is obtained. To carry this agenda further, we propose concept of “Dice-calibrated”, following the same philosophy of Fisher consistency or classification-calibration in Lin (2004); Zhang (2004); Bartlett et al. (2006). Intuitively, Dice-calibration is the weakest possible condition on a consistent segmentation method with respect to the Dice metric, this is, at population level, a method ultimately searches for the Bayes rule that achieves the optimal Dice metric.

To proceed, we denote $\mathbb{P}_{\mathbf{X}, \mathbf{Y}}$ as a probability measure of (\mathbf{X}, \mathbf{Y}) , \mathcal{P} as a class of all possible probability measures on (\mathbf{X}, \mathbf{Y}) , and \mathcal{D} as a class of all possible segmentation operators $\boldsymbol{\delta} : \mathbf{x} \in \mathbb{R}^d \rightarrow \boldsymbol{\delta}(\mathbf{x}) \in \{0, 1\}^d$. The definition of Dice-calibrated segmentation is given as follows.

Definition 7 (Dice-calibrated segmentation) Given $\gamma \geq 0$, a (population) segmentation method $\mathcal{M}_\gamma : \mathcal{P} \rightarrow \mathcal{D}$ is Dice-calibrated if, for any $\mathbb{P}_{\mathbf{X}, \mathbf{Y}} \in \mathcal{P}$,

$$\text{Dice}_\gamma(\mathcal{M}_\gamma(\mathbb{P}_{\mathbf{X}, \mathbf{Y}})) = \text{Dice}_\gamma(\boldsymbol{\delta}^*),$$

where $\boldsymbol{\delta}^*$ is the Bayes rule for Dice-segmentation defined in Theorem 1.

Now, we show that most existing loss functions, under the framework (2), are not Dice-calibrated.

Lemma 8 Given a loss function $l(\cdot, \cdot)$, define $\mathcal{M}_\gamma(\mathbb{P}_{\mathbf{X}, \mathbf{Y}})$ under the framework (2), that is,

$$\mathcal{M}_\gamma(\mathbb{P}_{\mathbf{X}, \mathbf{Y}})(\mathbf{x}) = \mathbf{1}(\tilde{\mathbf{q}}_l(\mathbf{x}) \geq 0.5), \quad \tilde{\mathbf{q}}_l = \underset{\mathbf{q}}{\operatorname{argmin}} \mathbb{E}(l(\mathbf{Y}, \mathbf{q}(\mathbf{X}))).$$

Then, $\mathcal{M}_\gamma(\mathbb{P}_{\mathbf{X}, \mathbf{Y}})$ is not Dice-calibrated for $\gamma = 0$ when $l(\cdot, \cdot)$ is the soft-Dice loss or any classification-calibrated loss, including the cross-entropy loss and the focal loss.

Lemma 8 indicates that the existing framework (2) with most losses ultimately yields a sub-optimal solution to Dice-segmentation, even if a “classification-calibrated” loss, such as the cross-entropy loss or the focal loss (Charoenphakdee et al., 2021), is used. Meanwhile, the result for the soft-Dice loss in Lemma 8 is in line with the empirical results in Bertels et al. (2019), where optimization with the soft-Dice loss can introduce a volumetric bias for tasks with high inherent

uncertainty. In sharp contrast, the proposed *RankDice* method is Dice-calibrated (Lemma 9) and its asymptotic convergence rate in terms of the Dice metric is provided in Theorem 10.

To proceed, we give the definition of *RankDice* at population level in Appendix B.1, which replaces the average in (5) by the population expectation. Moreover, the cross-entropy loss in (5) can be extended to an arbitrary *strictly proper* loss (Gneiting and Raftery, 2007). The most common strictly proper losses are the cross-entropy loss and the squared error loss.

Lemma 9 (Dice-calibrated) *The proposed RankDice framework with a strictly proper loss is Dice-calibrated.*

Next, we present an excess risk bound in terms of the Dice metric, that is, $\text{Dice}(\boldsymbol{\delta}^*) - \text{Dice}(\hat{\boldsymbol{\delta}})$.

Theorem 10 (Excess risk bounds) *Given $\gamma \geq 0$, let $\hat{\mathbf{q}}(\cdot)$ be an estimated probability of $\mathbf{p}(\cdot)$, and $\hat{\boldsymbol{\delta}}(\cdot)$ be the RankDice segmentation function defined in (7) based on $\hat{\mathbf{q}}(\cdot)$, then*

$$\text{Dice}_\gamma(\boldsymbol{\delta}^*) - \text{Dice}_\gamma(\hat{\boldsymbol{\delta}}) \leq C_1 \mathbb{E}_{\mathbf{X}} \|\hat{\mathbf{q}}(\mathbf{X}) - \mathbf{p}(\mathbf{X})\|_1, \quad (19)$$

where $C_1 > 0$ is a universal constant depending only on γ .

As indicated in Theorem 10, the excess risk of the Dice metric for the proposed *RankDice* framework is upper bounded by the total variation (TV) distance between the estimated probability $\hat{\mathbf{q}}$ and the true probability \mathbf{p} . Note that the Kullback-Leibler divergence (the excess risk for the cross-entropy) dominates the TV distance. It follows that if the KL divergence between p_j and \hat{q}_j goes to 0, then $\hat{\mathbf{q}}$ converges to \mathbf{p} in the TV sense, and so does $\text{Dice}_\gamma(\hat{\boldsymbol{\delta}})$ to $\text{Dice}_\gamma(\boldsymbol{\delta}^*)$.

Taken together, we present the rate of convergence for the empirical estimator obtained from the proposed *RankDice* framework (Steps 1-3) in Section 2.2.

Corollary 11 (Convergence rate) *Let $\hat{\mathbf{q}}(\cdot)$ and $\hat{\boldsymbol{\delta}}(\cdot)$ be obtained by the proposed RankDice framework (Steps 1-3) in Section 2.2, and*

$$\mathcal{E}_{CE}(\hat{\mathbf{q}}) := \mathbb{E} \left(l_{CE}(\mathbf{Y}, \hat{\mathbf{q}}(\mathbf{X})) \right) - \mathbb{E} \left(l_{CE}(\mathbf{Y}, \mathbf{p}(\mathbf{X})) \right) = O_P(\varepsilon_n),$$

where $l_{CE}(\cdot, \cdot)$ is defined in (3). Then,

$$\text{Dice}_\gamma(\boldsymbol{\delta}^*) - \text{Dice}_\gamma(\hat{\boldsymbol{\delta}}) = O_P(\sqrt{d} \varepsilon_n^{1/2}). \quad (20)$$

Note that \mathcal{E}_{CE} is the excess risk of the cross-entropy loss or the negative conditional log-likelihood in (5), and its asymptotics as well as a rate of convergence can be established based on statistical learning theory of empirical risk minimization (Pollard, 1984; Shen, 1997; Bartlett et al., 2005; Giné and Koltchinskii, 2006), which depends on the sample size and the complexity of the probability class. Then, the rate of convergence of the excess risk in terms of the Dice metric is obtained via (20). Note that both (19) and (20) are derived for a fixed dimension, and the upper bounds can be extended and improved when the dimension of segmentation grows with the sample size.

4.2 Relation between Dice and IoU metrics

In this section, we consider the relation and difference between Dice and IoU metrics, and present the Bayes rule for IoU-segmentation.

Lemma 12 *A segmentation rule δ^* is a global maximizer of $\text{IoU}_\gamma(\delta)$ if and only if it satisfies that*

$$\delta_j^*(\mathbf{x}) = \begin{cases} 1 & \text{if } p_j(\mathbf{x}) \text{ ranks top } \tau^*(\mathbf{x}), \\ 0 & \text{otherwise.} \end{cases}$$

The optimal volume $\tau^*(\mathbf{x})$ is given as

$$\tau^*(\mathbf{x}) = \underset{\tau \in \{0,1,\dots,d\}}{\operatorname{argmax}} \left(\sum_{j \in J_\tau(\mathbf{x})} p_j(\mathbf{x}) + \gamma \right) \sum_{l=0}^{d-\tau} \frac{1}{\tau + l + \gamma} \mathbb{P}(\Gamma_{-J_\tau(\mathbf{x})}(\mathbf{x}) = l), \quad (21)$$

where $J_\tau(\mathbf{x}) = \{j : \sum_{j'=1}^d \mathbb{I}(p_{j'}(\mathbf{x}) \geq p_j(\mathbf{x})) \leq \tau\}$ is the index set of the τ -largest conditional probabilities with $J_0(\mathbf{x}) = \emptyset$, and $\Gamma_{-J_\tau(\mathbf{x})}(\mathbf{x}) = \sum_{j' \notin J_\tau(\mathbf{x})} B_{j'}(\mathbf{x})$ is a Poisson-binomial random variable, and $B_j(\mathbf{x})$ is a Bernoulli random variable with the success probability $p_j(\mathbf{x})$.

According to Lemma 12, there is a substantial similarity between Dice-segmentation and IoU-segmentation in terms of the Bayes rule. On this ground, a consistent *RankIoU* framework is also developed based on a *plug-in* rule by replacing $\mathbf{p}(\mathbf{x})$ as $\hat{\mathbf{q}}(\mathbf{x})$; see Appendix B.2. Moreover, the concepts of IoU-calibrated and its excess risk bounds can be established in the same manner as for Dice-segmentation.

In contrast to *RankDice*, *RankIoU* involves the evaluation of $\mathbb{P}(\Gamma_{-J_\tau(\mathbf{x})}(\mathbf{x}) = l)$ in the volume estimation, in which the proposed blind approximation for *RankDice* is not applicable and the computation scheme of *RankIoU* might be relatively expensive in high-dimensional segmentation.

5. Numerical experiments

This section describes a set of simulations and real datasets that demonstrate the segmentation performance of the proposed *RankDice* and *mRankDice* frameworks compared with the existing *argmax*- and *thresholding*-based frameworks using various loss functions and network architectures. For illustration, the segmentation performances for all numerical experiments are evaluated by empirical Dice/IoU metrics with $\gamma = 0$, see Appendix A. For the mDice/mIoU metric, the class-specific weight is defined as in (15). All experiments are conducted using PyTorch and CUDA on an NVIDIA GeForce RTX 3080 GPU. All Python codes are available for download at our GitHub repository (<https://github.com/statmlben/rankseg>).

5.1 Simulation

In this section, we mainly compare the proposed *RankDice* framework with the *thresholding*-based framework (2) in various simulated examples. Note that for Dice-segmentation with binary outcomes, *threshold*- and *argmax*-based frameworks yield the same solution. Both frameworks require an estimation of conditional probability function in the first stage. Therefore, in order to convincingly demonstrate the difference between two frameworks, in our simulation, we assume the true

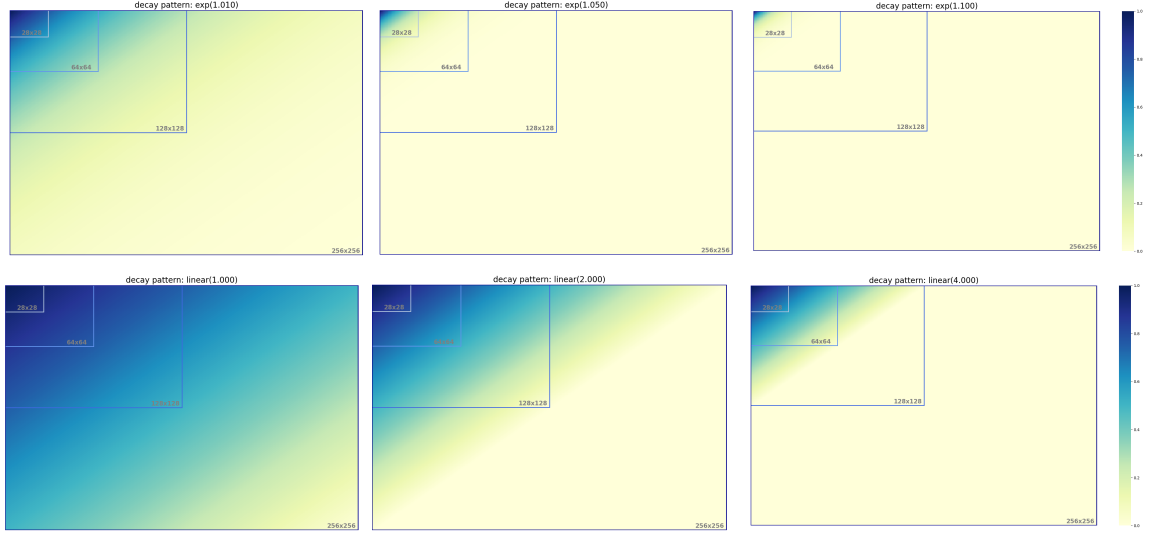


Figure 3: Simulation setting in Section 5.1 with different decay patterns and dimensions/shapes (28x28 - 256x256). **Upper panel.** Heatmaps for the simulated probabilities with exponential decay (base=1.01, 1.05, 1.10). **Lower panel.** Heatmaps for the simulated probabilities with linear decay (slope=1, 2, 4). The performances for the proposed *RankDice* and *thresholding*-based frameworks are summarized in Table 2.

conditional probabilities $p_j(\mathbf{x}) = \mathbb{P}(Y_j|\mathbf{x})$; $j = 1, \dots, d$ are perfectly estimated, and report the Dice metric of the downstream segmentation produced by two different frameworks.

To mimic the spatial smoothness in practical segmentation problem, especially for image segmentation, the simulated dataset based on matrix response ($d = W \times H$) is generated as follows. First, the true probability matrix $\mathbf{P} = (p_{wh})_{W \times H}$ are generated by two patterns:

- Exponential decay: $p_{wh} = \exp(-\beta(w+h))$, as visualized in the upper panel of Figure 3.
- Linear decay: $p_{wh} = 1 - \beta(w+h)/(W+H)$, as visualized in the lower panel of Figure 3.

Here β is a decay parameter. In our simulation, we consider $\beta = 1.01, 1.05, 1.10$ for exponential decay, and $\beta = 1, 2, 4$ for linear decay. For each case, four different dimensions are considered: $W = H = 28, 64, 128, 256$, and therefore d increases from 784 to 65,536. Then, the proposed *RankDice* framework and the *thresholding*-based framework (at 0.5) are conducted on the true probability matrix \mathbf{P} . Both decay scenarios are replicated 100 times, and the averaged Dice metrics and its standard errors are summarized in Table 2.

It is evident that *RankDice* significantly outperforms the *thresholding*-based framework in both decay scenarios with various dimensions. The amount of improvement is substantial, with the largest improvement of 57.3% in exponential decay with shape 256x256. Interestingly, the amount of improvement is gradually increased when the decay of probabilities becomes progressively faster. This suggests that the proposed *RankDice* might be even more advantageous in *well-separated segmentation*.

Decay (see Fig 3)	Shape	Threshold (at 0.5)	RankDice (our)
exp(1.01)	28x28	0.870(.000)	0.870(.000)
	64x64	0.669(.000)	0.714(.000)
	128x128	0.410(.000)	0.551(.000)
	256x256	0.286(.000)	0.450(.000)
exp(1.05)	28x28	0.427(.001)	0.551(.001)
	64x64	0.296(.001)	0.446(.001)
	128x128	0.276(.001)	0.427(.001)
	256x256	0.274(.001)	0.427(.001)
exp(1.10)	28x28	0.332(.002)	0.467(.002)
	64x64	0.301(.001)	0.439(.002)
	128x128	0.300(.002)	0.438(.002)
	256x256	0.298 (.002)	0.436(.002)
linear(1.00)	28x28	0.679(.001)	0.717(.001)
	64x64	0.672(.000)	0.711(.000)
	128x128	0.669(.000)	0.709(.000)
	256x256	0.668(.000)	0.707(.000)
linear(2.00)	28x28	0.578(.001)	0.647(.001)
	64x64	0.575(.001)	0.642(.001)
	128x128	0.573(.000)	0.638(.000)
	256x256	0.573(.000)	0.637(.000)
linear(4.00)	28x28	0.588(.003)	0.663(.002)
	64x64	0.580(.001)	0.646(.001)
	128x128	0.575(.001)	0.642(.001)
	256x256	0.574(.000)	0.639(.000)

Table 2: The averaged Dice metrics and its standard errors (in parentheses) of the proposed *RankDice* framework and the *thresholding*-based (or *argmax*-based) framework in simulated examples in Section 5.1.

5.2 Real datasets

This section examines the performance of the proposed *RankDice* framework in the PASCAL VOC 2012 (Everingham et al., 2012) and the fine-annotated CityScapes semantic segmentation benchmark (Cordts et al., 2016). Three different neural network architectures are considered: DeepLab-V3+ (Chen et al., 2018) with resnet101 as the backbone, PSPNet with resnet50 as the backbone, and FCN8 with resnet101 as the backbone. We report both mDice and mIoU metrics of the segmentation produced by Threshold, Argmax and RankDice on the *same* estimated network/probability. Note that only overlapping segmentation is considered.

Fine-annotated Cityscapes dataset contains 5,000 high quality pixel-level annotated images. For all methods, we employ SGD on the learning rate (lr) schedule `lr_schedule='poly'`, and the initial learning rate `initial_lr=0.01`, `weight_decay=100`, `momentum=0.9`, crop size 512x512,

batch size 6, and 300 epochs. The performance on validation set is measured in terms of the mDice and mIoU averaged across 19 object classes (Table 3).

Pascal VOC 2012 dataset contains 20 foreground object classes and one background class. The dataset contains 1,464 training and 1,449 validation pixel-level annotated images. We augment the dataset by using the additional annotations provided by Hariharan et al. (2011). For all methods, we employ SGD on the learning rate (lr) schedule `lr_schedule='poly'`, and the initial learning rate `initial_lr=0.01`, `weight_decay=100`, `momentum=0.9`, crop size 480x480, batch size 8, and an early stop with patient 10 based on validation loss. The performance on validation set is measured in terms of the mDice and mIoU averaged across the 20 object classes (Table 4). In this dataset, we also present a heatmap (Figure 4) for averaged minimal estimated probabilities for segmented features (i.e. $\hat{q}_{j_{\tau}}$) by the proposed *RankDice*, to highlight its difference to the *thresholding*-based framework.

Multiclass/multilabel Loss. In both datasets, we use six loss functions (including multiclass and multilabel losses) in the implementation, including the cross-entropy (CE), the focal loss (Focal), the binary cross-entropy (BCE), the soft-Dice loss (Soft-Dice), the binary soft-Dice loss (B-Soft-Dice), and the LovaszSoftmax loss (LovaszSoftmax). For multiclass losses, including CE, Focal, Soft-Dice, and LovaszSoftmax, we use the softmax function as the output layer activation function of a neural network. For multilabel losses, including BCE and B-Soft-Dice, we use the sigmoid function as the output layer activation function of a neural network.

Dice-segmentation based on a single class. For both datasets, when we focus on a single object class, it reduces to a Dice-segmentation with binary outcomes. To examine the performance for the proposed *RankDice* in binary segmentation, we also report the Dice/IoU metric for each label separately. In principle, we need to train a model only on the binary label for an object class, then produce the segmentation prediction by *thresholding* (or *argmax*) and *RankDice*. However, based on our empirical study, a model trained from full labels is significantly better than the one trained from a single binary label. We thus train a model based the same procedure in the aforementioned segmentation with multiclass/multilabel losses on full labels, and then produce the prediction based on the estimated probability for each object class separately. The best two performances (“PSPNet + CE” and “PSPNet + BCE”) for both datasets are summarized in Tables 5 and 6. The performance for other models and losses can be found in the supplementary. In Figure 5, we present the segmentation results on illustrative examples for all methods to demonstrate the difference between the proposed *RankDice* and the existing methods.

Overall, the empirical results show that the proposed *RankDice/mRankDice* framework yields good performance in both Fine-annotated Cityscapes dataset and Pascal VOC 2012 dataset. The major empirical conclusions on the proposed *RankDice* are listed as follows.

- As suggested in Tables 3 and 4, the proposed *RankDice* framework *consistently* outperforms the *threshold*-based and *argmax*-based frameworks based on the same trained model/network. The percentage of improvement on the best performance (for each framework) are 3.13% (over *threshold*) and 4.96% (over *argmax*) for CityScapes dataset (PSPNet + CE), and 3.87% (over *threshold*) and 2.91% (over *argmax*) for Pascal VOC 2021 dataset (PSPNet + CE/BCE).
- For Dice-segmentation based on a single class, as suggested in Tables 5 and 6, the proposed *RankDice* framework *consistently* outperforms the *threshold-largmax*-based framework for each class. The largest percentage of class-specific improvement in terms of the Dice metric

on the best performance (for each framework) is 23.6% for CityScapes dataset, and 26.9% for Pascal VOC 2021 dataset.

- The proposed *RankDice* works significantly better in “difficult” segmentation. As indicated in Tables 5 and 6, the improvements by *RankDice* are negative corrected with the resulting Dice/IoU metrics. It is also suggested by instance-level analysis in Figure 5, where we illustrate three images from classes *cat* (no improvement) and *chair* (26.9% improvement). As presented in all examples of *chair* and the last example of *cat*, the improvement is significant when segmentation is difficult (the target object is either nested or similar with other objects).
- As expected, the proposed *RankDice/mRankDice* performs well for strictly proper loss functions, including CE and BCE. In addition, we show that the performance is continuously improved compared with existing frameworks for some classification calibrated losses, such as the focal loss.
- Although the *RankDice/mRankDice* framework is developed for Dice/mDice optimization, the performance in terms of the IoU/mIoU metric is also consistently improved.

Moreover, we also present some important observations based on our experiments about losses, frameworks, and models.

- CE, Focal and BCE are the top three loss functions for Dice-segmentation. While some Dice approximating losses, such as Soft-Dice and binary Soft-Dice, usually lead to suboptimal solutions.
- It seems that the multiclass modeling and multiclass losses are more preferred for both datasets. Moreover, the *threshold*-based framework usually outperforms the *argmax*-based framework for both multiclass and multilabel losses.
- For multiclass losses, including CE Focal, Soft-Dice, and LovaszSoftmax, the Dice and IoU metrics are consistent, i.e., a higher Dice yields a higher IoU score. For multilabel losses, including BCE and B-Soft-Dice, there is a significant difference between Dice and IoU metrics.

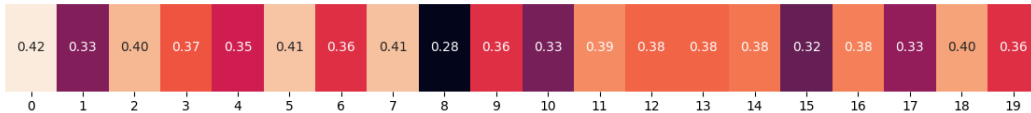


Figure 4: The heatmap for averaged (over all validation samples) minimal estimated probabilities for segmented features (i.e. the probability cutpoint $\hat{q}_{j_{\bar{\tau}}}$) by the proposed *RankDice* framework. Here, the x -axis indicates the class, and the results are provided by a PSPNet trained with the cross-entropy loss.

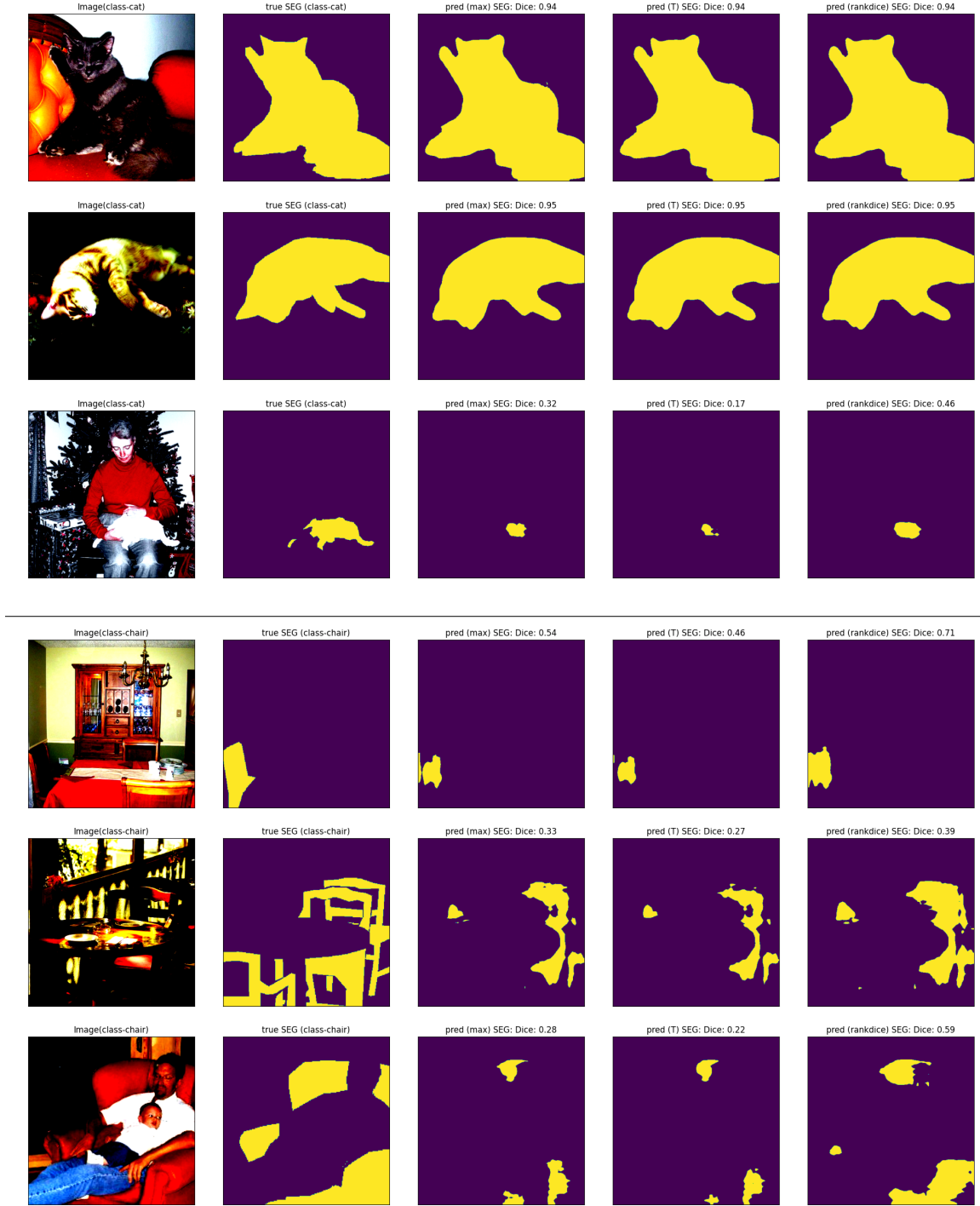


Figure 5: Comparison of segmentation results between the proposed method and existing methods for classes cat (upper panel) and chair (lower panel). Column 1 indicates original images, Column 2 indicates ground truths, and Columns 3-5 indicate the predicted segmentation produced by *argmax*, *thresholding*, and the proposed *RankDice*, respectively. The results are provided by a PSPNet trained with the cross-entropy loss.

Model	Loss	Threshold (at 0.5) (mDice, mIoU) ($\times .01$)	Argmax (mDice, mIoU) ($\times .01$)	mRankDice (our) (mDice, mIoU) ($\times .01$)
DeepLab-V3+ (resnet101)	CE	(56.00, 48.40)	(54.20, 46.60)	(57.80, 49.80)
	Focal	(54.10, 46.60)	(53.30, 45.60)	(56.50, 48.70)
	BCE	(49.80, 24.90)	(44.20, 22.10)	(54.00, 27.00)
	Soft-Dice	(39.50, 35.90)	(39.50, 35.90)	/
	B-Soft-Dice	(41.00, 20.50)	(27.60, 13.80)	/
	LovaszSoftmax	(55.20, 47.60)	(52.30, 45.10)	/
PSPNet (resnet50)	CE	(57.50, 49.60)	(56.50, 48.50)	(59.30, 51.00)
	Focal	(56.00, 48.20)	(55.80, 47.70)	(58.20, 50.00)
	BCE	(51.40, 25.70)	(47.60, 23.80)	(55.10, 27.60)
	Soft-Dice	(49.10, 43.50)	(48.70, 43.20)	/
	B-Soft-Dice	(46.30, 23.10)	(32.70, 16.40)	/
	LovaszSoftmax	(56.80, 48.90)	(55.40, 47.70)	/
FCN8 (resnet101)	CE	(51.40, 43.70)	(50.50, 42.60)	(53.50, 45.30)
	Focal	(48.50, 41.20)	(49.60, 41.60)	(51.50, 43.70)
	BCE	(39.40, 19.70)	(39.40, 19.70)	(41.30, 20.60)
	Soft-Dice	(28.30, 24.30)	(28.30, 24.30)	/
	B-Soft-Dice	(29.10, 14.60)	(29.10, 14.60)	/
	LovaszSoftmax	(48.10, 40.40)	(42.90, 35.80)	/

Table 3: Averaged mDice and mIoU metrics of *Threshold*, *Argmax*, and the proposed *mRankDice* based on state-of-the-art models/losses on **Fine-annotated CityScapes** *val* set. “/” indicates not applicable since the proposed *RankDice/mRankDice* requires a strictly proper loss. The best performance in each model/loss is bold-faced.

6. Conclusions and future work

In this paper, we proposed a Dice-calibrated ranking-based framework for segmentation with respect to the Dice metric. We have developed general theoretical results, including excess risk bounds and a rate of convergence, as well as efficient GPU-enabled algorithms for the proposed framework. Empirical experiments suggested that this framework performs consistently well on a variety of segmentation benchmarks and state-of-the-art deep learning architectures.

Our results in this paper cover overlapping (allowing) segmentation, and it would be interesting to develop a scalable approximating algorithm to utilize the proposed framework in the non-overlapping setting. Moreover, it is also of interest to incorporate learning-to-rank approaches to our framework (Cl  men  on et al., 2008; Chapelle and Chang, 2011).

Acknowledgments

We would like to acknowledge support for this project from the CUHK direct fund.

Model	Loss	Threshold (at 0.5) (mDice, mIoU) ($\times .01$)	Argmax (mDice, mIoU) ($\times .01$)	mRankDice (our) (mDice, mIoU) ($\times .01$)
DeepLab-V3+ (resnet101)	CE	(63.60, 56.70)	(61.90, 55.30)	(64.01, 57.01)
	Focal	(62.70, 55.01)	(60.50, 53.20)	(62.90, 55.10)
	BCE	(63.30, 31.70)	(59.90, 29.90)	(64.60, 32.30)
	Soft-Dice	—	—	/
	B-Soft-Dice	—	—	/
	LovaszSoftmax	(57.70, 51.60)	(56.20, 50.30)	/
PSPNet (resnet50)	CE	(64.60, 57.10)	(63.20, 55.90)	(65.40, 57.80)
	Focal	(64.00, 56.10)	(63.90, 56.10)	(66.60, 58.50)
	BCE	(64.20, 32.10)	(65.20, 32.60)	(67.10, 33.50)
	Soft-Dice	(59.60, 54.00)	(58.80, 53.20)	/
	B-Soft-Dice	(63.30, 31.60)	(54.00, 27.00)	/
	LovaszSoftmax	(62.00, 55.20)	(60.80, 54.10)	/
FCN8 (resnet101)	CE	(49.50, 41.90)	(45.30, 38.40)	(50.40, 42.70)
	Focal	(50.40, 41.80)	(47.20, 39.30)	(51.50, 42.50)
	BCE	(46.20, 23.10)	(44.20, 22.10)	(47.70, 23.80)
	Soft-Dice	—	—	/
	B-Soft-Dice	—	—	/
	LovaszSoftmax	(39.80, 34.30)	(37.30, 32.20)	/

Table 4: Averaged mDice and mIoU of *threshold*, *argmax*, and the proposed *mRankDice* based on state-of-the-art models/losses on **PASCAL VOC 2012** *val* set. “—” indicates that either the performance is significantly worse or the training is unstable, and “/” indicates not applicable since the proposed *RankDice/mRankDice* requires a strictly proper loss. The best performance in each model-loss pair is bold-faced.

A. Empirical evaluation of the Dice metric

Recall the definition of the Dice metric in (1), its empirical evaluation based on a validation/testing dataset $(\tilde{\mathbf{x}}_i, \tilde{\mathbf{y}}_i)_{i=1, \dots, m}$, can be written as:

$$\widehat{\text{Dice}}_\gamma(\boldsymbol{\delta}) = \frac{1}{m} \sum_{i=1}^m \frac{2\tilde{\mathbf{y}}_i^\top \boldsymbol{\delta}(\tilde{\mathbf{x}}_i) + \gamma}{\|\tilde{\mathbf{y}}_i\|_1 + \|\boldsymbol{\delta}(\tilde{\mathbf{x}}_i)\|_1 + \gamma} = \frac{1}{m} \sum_{i=1}^m \frac{2\text{TP}_i + \gamma}{2\text{TP}_i + \text{FP}_i + \text{FN}_i + \gamma}, \quad (22)$$

where TP_i , FP_i and FN_i are defined at the instance level. In general, the empirical Dice metric $\widehat{\text{Dice}}_\gamma(\boldsymbol{\delta})$ is not equal to the evaluation criteria used in some literature:

$$\widehat{\text{Dice}}_\gamma(\boldsymbol{\delta}) \neq \frac{\frac{1}{m} \sum_{i=1}^m 2\tilde{\mathbf{y}}_i^\top \boldsymbol{\delta}(\tilde{\mathbf{x}}_i) + \gamma}{\frac{1}{m} \sum_{i=1}^m \|\tilde{\mathbf{y}}_i\|_1 + \frac{1}{m} \sum_{i=1}^m \|\boldsymbol{\delta}(\tilde{\mathbf{x}}_i)\|_1 + \gamma} \xrightarrow{p} \frac{\mathbb{E}(2\mathbf{Y}^\top \boldsymbol{\delta}(\mathbf{X})) + \gamma}{\mathbb{E}(\|\mathbf{Y}\|_1) + \mathbb{E}(\|\boldsymbol{\delta}(\mathbf{X})\|_1) + \gamma}. \quad (23)$$

Here \xrightarrow{p} denotes convergence in probability following from the law of large numbers and Slutsky’s theorem. Clearly, both empirical and population evaluations in (23) do not match with the empirical Dice in (22) and the population Dice in (1). Although the empirical evaluation in (23) is widely used, it inherently discounts the effects of instances with small segmented features/pixels, leading to bias in the empirical evaluation. Therefore, it is highly recommended using the empirical Dice in (22) in implementation, and our numerical results in Section 5 are reported based on (22).

Object class	Threshold/Argmax (Dice, IoU) ($\times .01$)			RankDice (our) (Dice, IoU) ($\times .01$)			imps. (best vs. best) (Dice)
	CE	Focal	BCE	CE	Focal	BCE	
road	(85.7, 77.2)	(86.1, 77.9)	(92.2, 46.1)	(85.6, 77.1)	(86.0, 77.7)	(92.2, 46.1)	\sim
sidewalk	(57.3, 47.8)	(53.6, 43.8)	(43.8, 21.9)	(60.8, 50.8)	(58.7, 48.4)	(54.0, 27.0)	6.1%
building	(84.6, 76.2)	(83.4, 74.8)	(79.4, 39.7)	(85.1, 76.7)	(83.6, 74.7)	(82.1, 41.0)	\sim
wall	(17.4, 13.6)	(16.1, 12.4)	(04.9, 02.4)	(21.0, 16.4)	(21.5, 16.8)	(08.3, 04.2)	23.6%
fence	(14.7, 10.9)	(12.4, 08.9)	(15.2, 07.6)	(15.8, 11.7)	(13.7, 09.8)	(19.1, 09.5)	25.7%
pole	(41.9, 29.0)	(34.7, 23.4)	(27.1, 13.5)	(46.0, 31.7)	(35.6, 23.1)	(36.4, 18.2)	9.8%
traffic light	(34.9, 26.5)	(31.5, 24.0)	(18.7, 09.4)	(37.4, 28.3)	(33.5, 24.7)	(21.3, 10.6)	7.2%
traffic sign	(49.9, 39.0)	(45.9, 35.1)	(35.3, 17.6)	(51.4, 40.1)	(46.6, 35.1)	(39.6, 19.8)	3.0%
vegetation	(90.2, 84.1)	(90.2, 83.8)	(89.0, 44.5)	(90.3, 84.1)	(89.6, 82.8)	(89.4, 44.7)	\sim
terrain	(25.7, 20.1)	(24.1, 18.5)	(19.8, 09.9)	(29.4, 23.1)	(28.7, 22.7)	(25.3, 12.7)	14.4%
sky	(83.6, 77.0)	(82.0, 75.2)	(80.1, 40.0)	(84.5, 77.8)	(83.1, 76.2)	(80.7, 40.3)	1.1%
person	(45.1, 36.3)	(42.6, 34.1)	(32.8, 16.4)	(49.5, 40.0)	(47.6, 38.2)	(38.6, 19.3)	9.8%
rider	(35.1, 27.3)	(31.2, 24.0)	(18.6, 09.3)	(37.2, 29.2)	(33.9, 26.3)	(24.0, 12.0)	6.0%
car	(84.1, 76.9)	(83.4, 76.2)	(80.8, 40.4)	(84.0, 76.6)	(81.8, 74.0)	(81.2, 40.6)	\sim
truck	(24.7, 21.9)	(25.6, 22.7)	(21.8, 10.9)	(26.6, 23.3)	(28.1, 24.8)	(26.8, 13.4)	9.8%
bus	(46.8, 42.2)	(48.8, 43.8)	(36.3, 18.2)	(51.3, 46.5)	(51.5, 46.8)	(39.2, 19.6)	5.5%
train	(34.9, 30.7)	(36.3, 31.0)	(33.8, 16.9)	(35.8, 31.5)	(37.3, 32.2)	(34.7, 17.4)	2.8%
motorcycle	(19.7, 15.8)	(20.4, 16.1)	(07.0, 03.5)	(22.2, 17.7)	(21.1, 16.8)	(08.7, 04.4)	8.8%
bicycle	(41.4, 32.5)	(42.1, 32.9)	(32.9, 16.5)	(41.9, 32.6)	(42.0, 32.5)	(36.7, 18.4)	\sim

Table 5: Averaged class-specific Dice and IoU metrics of *Threshold/Argmax*, and the proposed *RankDice* based on various losses of PSPNet + resnet50 on **Fine-annotated CityScapes val** set. The class-specific improvement in terms of the Dice metric of the proposed RankDice framework is computed in “imps.”, where \sim indicates that the difference between *Threshold/Argmax* and the proposed *RankDice* is smaller than 1.0%.

B. Auxiliary definitions

B.1 Population RankDice

In this section, we present the definition of population *RankDice*. In other words, we work with population of random variables (\mathbf{X}, \mathbf{Y}) , and assume that \mathcal{Q} is the set of all measurable probabilities. **Step 1 (Conditional probability estimation)**: Estimate the conditional probability based on a strictly proper loss $l(\cdot, \cdot)$:

$$\hat{\mathbf{q}}(\mathbf{x}) = \underset{\mathbf{q} \in \mathcal{Q}}{\operatorname{argmin}} \mathbb{E}(l(\mathbf{Y}, \mathbf{q}(\mathbf{X}))). \quad (24)$$

Step 2 (Ranking): Given a new instance \mathbf{x} , sort its estimated conditional probabilities decreasingly, and denote the corresponding indices as j_1, \dots, j_d , that is, $\hat{q}_{j_1}(\mathbf{x}) \geq \hat{q}_{j_2}(\mathbf{x}) \geq \dots \geq \hat{q}_{j_d}(\mathbf{x})$.

Step 3 (Volume estimation): From (4), we estimate the volume $\hat{\tau}(\mathbf{x})$ by replacing the true conditional probability $\mathbf{p}(\mathbf{x})$ by the estimated one $\hat{\mathbf{q}}(\mathbf{x})$:

$$\hat{\tau}(\mathbf{x}) = \underset{\tau \in \{0, \dots, d\}}{\operatorname{argmax}} \sum_{s=1}^{\tau} \sum_{l=0}^{d-1} \frac{2}{\tau + l + \gamma + 1} \hat{q}_{j_s}(\mathbf{x}) \mathbb{P}(\hat{\Gamma}_{-j_s}(\mathbf{x}) = l) + \sum_{l=0}^d \frac{\gamma}{\tau + l + \gamma} \mathbb{P}(\hat{\Gamma}(\mathbf{x}) = l),$$

where $\hat{\Gamma}(\mathbf{x}) = \sum_{j=1}^d \hat{B}_j(\mathbf{x})$ and $\hat{\Gamma}_{-j_s}(\mathbf{x}) = \sum_{j \neq j_s} \hat{B}_j(\mathbf{x})$ are Poisson-binomial random variables, and $\hat{B}_j(\mathbf{x})$ is a Bernoulli random variable with the success probability $\hat{q}_j(\mathbf{x})$.

Object class	Threshold/Argmax (Dice, IoU) ($\times .01$)			RankDice (our) (Dice, IoU) ($\times .01$)			imps. (best vs. best) (Dice)
	CE	Focal	BCE	CE	Focal	BCE	
Aeroplane	(71.2, 63.4)	(68.4, 59.2)	(72.9, 36.5)	(71.3, 63.4)	(72.7, 64.1)	(75.3, 37.6)	3.3%
Bicycle	(37.1, 25.9)	(19.6, 12.4)	(14.6, 7.30)	(38.7, 27.3)	(30.5, 20.6)	(23.1, 11.5)	4.3%
Bird	(76.0, 68.2)	(74.3, 65.2)	(74.2, 37.1)	(76.6, 68.7)	(75.8, 66.4)	(76.3, 38.1)	~
Boat	(51.1, 42.7)	(59.5, 49.1)	(55.5, 27.8)	(51.3, 42.9)	(61.9, 51.5)	(61.0, 30.5)	4.0%
Bottle	(42.8, 35.8)	(36.2, 30.0)	(39.1, 19.6)	(44.2, 36.8)	(37.6, 31.4)	(41.1, 20.6)	3.3%
Bus	(72.8, 68.3)	(72.3, 67.5)	(74.8, 37.4)	(74.1, 69.6)	(73.5, 68.8)	(75.9, 37.9)	1.5%
Car	(53.5, 47.5)	(51.1, 45.6)	(48.9, 24.4)	(55.0, 49.0)	(53.6, 47.9)	(51.7, 25.9)	2.7%
Cat	(75.0, 69.2)	(74.1, 67.9)	(73.1, 36.6)	(75.5, 69.7)	(75.4, 68.7)	(75.1, 37.6)	~
Chair	(17.5, 12.8)	(16.7, 11.6)	(10.2, 5.10)	(19.6, 14.4)	(22.2, 16.1)	(14.5, 7.30)	26.9%
Cow	(65.3, 58.6)	(60.1, 53.7)	(64.9, 32.4)	(66.5, 59.9)	(62.3, 56.0)	(68.4, 34.2)	4.8%
Diningtable	(32.9, 27.5)	(33.6, 27.4)	(31.7, 15.9)	(34.5, 29.2)	(38.6, 32.4)	(35.3, 17.6)	14.9%
Dog	(64.6, 57.9)	(71.0, 63.4)	(71.7, 35.9)	(65.5, 58.7)	(72.5, 64.9)	(74.4, 37.2)	3.8%
Horse	(63.9, 55.3)	(67.3, 58.3)	(67.0, 33.5)	(65.3, 56.6)	(69.5, 60.1)	(70.9, 35.4)	5.4%
Motorbike	(69.7, 60.6)	(65.5, 56.7)	(66.9, 33.5)	(71.6, 62.6)	(67.0, 57.9)	(70.1, 35.1)	2.7%
Person	(67.0, 57.7)	(65.0, 55.4)	(67.4, 33.7)	(67.4, 58.1)	(67.2, 57.6)	(69.7, 34.8)	3.4%
Pottedplant	(26.9, 20.2)	(22.4, 17.3)	(25.5, 12.8)	(29.1, 22.0)	(26.9, 20.7)	(28.6, 14.3)	8.2%
Sheep	(53.9, 47.4)	(62.8, 55.4)	(62.1, 31.1)	(54.3, 47.9)	(66.0, 58.6)	(66.9, 33.4)	6.5%
Sofa	(29.8, 25.0)	(29.8, 24.4)	(33.7, 16.8)	(32.0, 26.9)	(34.6, 29.0)	(38.9, 19.4)	14.5%
Train	(77.7, 71.0)	(75.8, 68.9)	(80.3, 40.1)	(77.9, 71.1)	(77.3, 70.4)	(82.1, 41.1)	2.2%
Tvmonitor	(48.4, 41.4)	(50.7, 41.6)	(53.7, 26.8)	(49.2, 42.0)	(54.1, 45.4)	(56.4, 28.2)	5.0%

Table 6: Class-specific Dice and IoU of *Threshold/Argmax*, and the proposed *RankDice* based on various losses of PSPNet + resnet50 on **PASCAL VOC 2012** *val* set. The class-specific improvement in terms of the Dice metric of the proposed *RankDice* framework is computed in “imps.”, where ~ indicates that the difference between *Threshold/Argmax* and the proposed *RankDice* is smaller than 1.0%.

B.2 RankIoU

Given a training dataset $(\mathbf{x}_i, \mathbf{y}_i)_{i=1}^n$, where $\mathbf{x}_i \in \mathbb{R}^d$ and $\mathbf{y}_i \in \{0, 1\}^d$ are the features and true labels, the proposed RankIoU is defined as follows.

Step 1 (Conditional probability estimation): Estimate the conditional probabilities based on multilabel logistic regression (binary cross entropy):

$$\hat{\mathbf{q}}(\mathbf{x}) = \underset{\mathbf{q} \in \mathcal{Q}}{\operatorname{argmin}} \sum_{i=1}^n \sum_{j=1}^d \left(y_{ij} \log(q_j(\mathbf{x}_i)) + (1 - y_{ij}) \log(1 - q_j(\mathbf{x}_i)) \right) + \lambda \|\mathbf{q}\|^2,$$

where \mathcal{Q} is a collection of candidate probability functions, $\|\mathbf{q}\|$ is a regularization for a candidate function, and $\lambda > 0$ is a hyperparameter to balance the loss and regularization and avoid overfitting.

Step 2 (Ranking): Given a new instance \mathbf{x} , sort its estimated conditional probabilities decreasingly, and denote the corresponding indices as j_1, \dots, j_d , that is, $\hat{q}_{j_1}(\mathbf{x}) \geq \hat{q}_{j_2}(\mathbf{x}) \geq \dots \geq \hat{q}_{j_d}(\mathbf{x})$.

Step 3 (Volume estimation): From (4), we estimate the volume $\hat{\tau}(\mathbf{x})$ by replacing the true conditional probability $\mathbf{p}(\mathbf{x})$ with the estimated one $\hat{\mathbf{q}}(\mathbf{x})$:

$$\hat{\tau}(\mathbf{x}) = \underset{\tau \in \{0, 1, \dots, d\}}{\operatorname{argmax}} \left(\sum_{j \in J_\tau(\mathbf{x})} \hat{q}_j(\mathbf{x}) + \gamma \right) \sum_{l=0}^{d-\tau} \frac{1}{\tau + l + \gamma} \mathbb{P}(\hat{\Gamma}_{-J_\tau(\mathbf{x})}(\mathbf{x}) = l),$$

where $\hat{\Gamma}_{-J_\tau(\mathbf{x})}(\mathbf{x}) = \sum_{j \notin J_\tau(\mathbf{x})} \hat{B}_j(\mathbf{x})$ is a Poisson-binomial random variable, and $\hat{B}_j(\mathbf{x})$ are independent Bernoulli random variables with success probabilities $\hat{q}_j(\mathbf{x})$; for $j = 1, \dots, d$.

Finally, the predicted segmentation $\widehat{\boldsymbol{\delta}}(\mathbf{x}) = (\widehat{\delta}_1(\mathbf{x}), \dots, \widehat{\delta}_d(\mathbf{x}))^\top$ is produced by taking the top- $\widehat{\tau}(\mathbf{x})$ conditional probabilities:

$$\widehat{\delta}_j(\mathbf{x}) = 1, \text{ if } j \in \{j_1, \dots, j_{\widehat{\tau}(\mathbf{x})}\}; \quad \widehat{\delta}_j(\mathbf{x}) = 0, \text{ otherwise.}$$

B.3 Poisson-binomial distribution

The Poisson binomial distribution is the discrete probability distribution of a sum of independent non-identical Bernoulli trials. Specifically, suppose B_1, \dots, B_d are independent Bernoulli random variables, with probabilities of success $\mathbf{p} = (p_1, \dots, p_d)^\top$, then $\Gamma = \sum_{j=1}^d B_j$ is a Poisson-Binomial random variable with parameter \mathbf{p} , denoted as $\Gamma \sim \text{PB}(\mathbf{p})$, and its probability mass function is:

$$\mathbb{P}(\Gamma = l) = \sum_{\mathbf{b}: \|\mathbf{b}\|_1 = l} \prod_{j=1}^d (b_j p_j + (1 - b_j)(1 - p_j)),$$

where $\mathbf{b} = (b_1, \dots, b_d)^\top \in \{0, 1\}^d$. Moreover, the mean, variance, and skewness for $\Gamma \sim \text{PB}(\mathbf{p})$ are listed as follows.

$$\mu := \mathbb{E}(\Gamma) = \sum_{j=1}^d p_j, \quad \sigma^2 := \text{Var}(\Gamma) = \sum_{j=1}^d p_j(1 - p_j), \quad \eta := \text{Skew}(\Gamma) = \frac{1}{\sigma^3} \sum_{j=1}^d p_j(1 - p_j)(1 - 2p_j).$$

C. Technical proofs

C.1 Proof of Theorem 1

Proof It suffices to consider the point-wise maximization:

$$\boldsymbol{\delta}^*(\mathbf{x}) = \underset{\mathbf{v} \in \{0,1\}^d}{\text{argmax}} \text{Dice}_\gamma(\mathbf{v}|\mathbf{x}), \quad \text{Dice}_\gamma(\mathbf{v}|\mathbf{x}) = \mathbb{E} \left(\frac{2\mathbf{Y}^\top \mathbf{v} + \gamma}{\|\mathbf{Y}\|_1 + \|\mathbf{v}\|_1 + \gamma} \middle| \mathbf{X} = \mathbf{x} \right).$$

Let $\mathbf{y}_{-j} = (y_1, \dots, y_{j-1}, y_{j+1}, \dots, y_d)^\top$, $I(\mathbf{v}) = I(\boldsymbol{\delta}(\mathbf{x})) = \{j : v_j = 1\}$ be the index set of segmented features by $\boldsymbol{\delta}(\mathbf{x})$, and $\|\mathbf{v}\|_1 = \tau$, we have

$$\text{Dice}_\gamma(\mathbf{v}|\mathbf{x}) = \mathbb{E} \left(\frac{2\mathbf{Y}^\top \mathbf{v}}{\|\mathbf{Y}\|_1 + \tau + \gamma} \middle| \mathbf{X} = \mathbf{x} \right) + \mathbb{E} \left(\frac{\gamma}{\|\mathbf{Y}\|_1 + \tau + \gamma} \middle| \mathbf{X} = \mathbf{x} \right).$$

Note that the second term is only related to τ , and the first term can be rewritten as:

$$\begin{aligned} \mathbb{E} \left(\frac{2\mathbf{Y}^\top \mathbf{v}}{\|\mathbf{Y}\|_1 + \tau + \gamma} \middle| \mathbf{X} = \mathbf{x} \right) &= \sum_{\mathbf{y} \in \{0,1\}^d} \frac{2\mathbf{y}^\top \mathbf{v} \mathbb{P}(\mathbf{Y} = \mathbf{y}|\mathbf{x})}{\tau + \|\mathbf{y}\|_1 + \gamma} = \sum_{\mathbf{y} \in \{0,1\}^d} \sum_{j=1}^d \frac{2y_j v_j \mathbb{P}(\mathbf{Y} = \mathbf{y}|\mathbf{x})}{\tau + \|\mathbf{y}\|_1 + \gamma} \\ &= \sum_{j \in I(\mathbf{v})} \sum_{\mathbf{y} \in \{0,1\}^d} \frac{2y_j \mathbb{P}(\mathbf{Y} = \mathbf{y}|\mathbf{x})}{\tau + \|\mathbf{y}\|_1 + \gamma} = \sum_{j \in I(\mathbf{v})} \sum_{\substack{\mathbf{y}_{-j} \in \{0,1\}^{d-1} \\ y_j = 1}} \frac{2\mathbb{P}(\mathbf{Y} = \mathbf{y}|\mathbf{x})}{\tau + \|\mathbf{y}\|_1 + \gamma} = \sum_{j \in I(\mathbf{v})} s_j(\tau). \end{aligned} \tag{25}$$

As indicated in (25), when τ is given, $\text{Dice}_\gamma(\mathbf{v}|\mathbf{x})$ is an additive function with respect to $j \in I(\mathbf{v})$. Therefore, maximizing $\text{Dice}_\gamma(\mathbf{v}|\mathbf{x})$ suffices to find the indices of top τ largest $s_j(\tau)$. Toward this

end, we consider the differenced score function:

$$\begin{aligned}
 D_{jj'}(\tau) &= s_j(\tau) - s_{j'}(\tau) = \sum_{\substack{\mathbf{y}_{-j} \in \{0,1\}^{d-1} \\ y_j=1}} \frac{2\mathbb{P}(\mathbf{Y}=\mathbf{y}|\mathbf{x})}{\tau + \|\mathbf{y}\|_1 + \gamma} - \sum_{\substack{\mathbf{y}_{-j'} \in \{0,1\}^{d-1} \\ y_{j'}=1}} \frac{2\mathbb{P}(\mathbf{Y}=\mathbf{y}|\mathbf{x})}{\tau + \|\mathbf{y}\|_1 + \gamma} \\
 &= \sum_{\substack{\mathbf{y}_{-jj'} \in \{0,1\}^{d-2} \\ y_j=1, y_{j'}=0}} \frac{2\mathbb{P}(\mathbf{Y}=\mathbf{y}|\mathbf{x})}{\tau + \|\mathbf{y}\|_1 + \gamma} - \sum_{\substack{\mathbf{y}_{-jj'} \in \{0,1\}^{d-2} \\ y_j=0, y_{j'}=1}} \frac{2\mathbb{P}(\mathbf{Y}=\mathbf{y}|\mathbf{x})}{\tau + \|\mathbf{y}\|_1 + \gamma} \\
 &= \sum_{\substack{\mathbf{y}_{-jj'} \in \{0,1\}^{d-2} \\ y_j=1, y_{j'}=0}} \frac{2\prod_{i \neq \{j, j'\}} \mathbb{P}(Y_i = y_i|\mathbf{x}) \mathbb{P}(Y_j = 1|\mathbf{x}) \mathbb{P}(Y_{j'} = 0|\mathbf{x})}{\tau + 1 + \|\mathbf{y}_{jj'}\|_1 + \gamma} \\
 &\quad - \sum_{\substack{\mathbf{y}_{-jj'} \in \{0,1\}^{d-2} \\ y_j=0, y_{j'}=1}} \frac{2\prod_{i \neq \{j, j'\}} \mathbb{P}(Y_i = y_i|\mathbf{x}) \mathbb{P}(Y_j = 0|\mathbf{x}) \mathbb{P}(Y_{j'} = 1|\mathbf{x})}{\tau + 1 + \|\mathbf{y}_{jj'}\|_1 + \gamma} \\
 &= (\mathbb{P}(Y_j = 1|\mathbf{x}) - \mathbb{P}(Y_{j'} = 1|\mathbf{x})) \sum_{\mathbf{y}_{-jj'} \in \{0,1\}^{d-2}} \frac{2\prod_{i \neq \{j, j'\}} \mathbb{P}(Y_i = y_i|\mathbf{x})}{\tau + 1 + \|\mathbf{y}_{jj'}\|_1 + \gamma}, \tag{26}
 \end{aligned}$$

where $\mathbf{y}_{-jj'}$ is \mathbf{y} removing y_j and $y_{j'}$, the second last inequality follows from the conditional independence of Y_j and $Y_{j'}$ given \mathbf{X} for any pair j and j' . According to (26), we have

$$D_{jj'}(\tau) \geq 0 \iff \mathbb{P}(Y_j = 1|\mathbf{x}) - \mathbb{P}(Y_{j'} = 1|\mathbf{x}) \geq 0,$$

thus sorting $s_j(\tau)$ is equivalent to sorting $\mathbb{P}(Y_j = 1|\mathbf{x})$ for any given τ . Let $J_\tau = \{j : \sum_{j'=1}^d \mathbf{1}(\mathbb{P}(Y_{j'} = 1|\mathbf{x}) \geq \mathbb{P}(Y_j = 1|\mathbf{x})) \leq \tau\}$ be the index set of the τ -largest conditional probabilities, it suffices to solve

$$\begin{aligned}
 \tau^* &= \operatorname{argmax}_{\tau=0, \dots, d} \sum_{j \in J_\tau} \mathbb{E}\left(\frac{2Y_j}{\|\mathbf{Y}\|_1 + \tau + \gamma}\right) + \mathbb{E}\left(\frac{\gamma}{\|\mathbf{Y}\|_1 + \tau + \gamma}\right) \\
 &= \operatorname{argmax}_{\tau=0, \dots, d} \sum_{j \in J_\tau} \sum_{l=0}^{d-1} \frac{p_j(\mathbf{x})}{\tau + l + \gamma + 1} \mathbb{P}(\|\mathbf{Y}_{-j}\|_1 = l | \mathbf{X} = \mathbf{x}) + \sum_{l=0}^d \frac{\gamma}{\tau + l + \gamma} \mathbb{P}(\|\mathbf{Y}\|_1 = l | \mathbf{X} = \mathbf{x}),
 \end{aligned}$$

where $\|\mathbf{Y}_{-j}\|_1 = \sum_{j' \neq j} Y_{j'}$ is a Poisson-binomial random variable with success probabilities $\mathbf{p}_{-j}(\mathbf{x})$, since Y_j ($j = 1, \dots, d$) is an independent Bernoulli random variable given $\mathbf{X} = \mathbf{x}$. The desirable result then follows. \blacksquare

C.2 Proof of Lemma 2

Proof To proceed, we denote $\xi_l(\mathbf{x}) = \mathbb{P}(\widehat{\Gamma}(\mathbf{x}) = l)$, and $\xi_{jl}(\mathbf{x}) = \mathbb{P}(\widehat{\Gamma}_{-j}(\mathbf{x}) = l)$, and $\bar{\pi}_\tau = \bar{\omega}_\tau(\mathbf{x}) + \bar{v}_\tau(\mathbf{x})$. For simplicity in presentation, we assume that $\widehat{q}_1(\mathbf{x}) \geq \dots \geq \widehat{q}_d(\mathbf{x})$. Then, for any $\tau' > \tau$,

since $\bar{v}_\tau \geq \bar{v}_{\tau'}$, and

$$\begin{aligned}
 \frac{\bar{\pi}_\tau(\mathbf{x}) - \bar{\pi}_{\tau'}(\mathbf{x})}{\tau' - \tau} &\geq \sum_{j=1}^{\tau} \hat{q}_j(\mathbf{x}) \sum_{l=0}^{d-1} \frac{\xi_{jl}(\mathbf{x})}{(\tau + l + 1 + \gamma)(\tau' + l + 1 + \gamma)} - \frac{1}{\tau' - \tau} \sum_{j=\tau+1}^{\tau'} \hat{q}_j(\mathbf{x}) \sum_{l=0}^{d-1} \frac{\xi_{jl}(\mathbf{x})}{\tau' + l + \gamma + 1} \\
 &\geq \sum_{j=1}^{\tau} \hat{q}_j(\mathbf{x}) \sum_{l=0}^{d-1} \frac{\xi_{\tau l}(\mathbf{x})}{(\tau + l + \gamma + 1)(\tau' + l + \gamma + 1)} - \hat{q}_{\tau+1}(\mathbf{x}) \sum_{l=0}^{d-1} \frac{\xi_{\tau l}(\mathbf{x})}{\tau' + l + \gamma + 1} \\
 &\geq \hat{q}_{\tau+1}(\mathbf{x}) \sum_{l=0}^{d-1} \frac{(\tau + \gamma + d)\xi_{\tau l}(\mathbf{x})}{(\tau + l + \gamma + 1)(\tau' + l + \gamma + 1)} - \hat{q}_{\tau+1}(\mathbf{x}) \sum_{l=0}^{d-1} \frac{\xi_{\tau l}(\mathbf{x})}{\tau' + l + \gamma + 1} \geq 0,
 \end{aligned} \tag{27}$$

where the first inequality follows from Lemma 14 with $\zeta_l = (\tau + l + \gamma + 1)(\tau' + l + \gamma + 1)$ and $\xi_l = \tau' + l + \gamma + 1$, and $\hat{q}_1(\mathbf{x}) \geq \dots \geq \hat{q}_\tau(\mathbf{x}) \geq \dots \geq \hat{q}_{\tau'}(\mathbf{x})$, and the third inequality follows from the condition that $\sum_{j=1}^{\tau} \hat{q}_j(\mathbf{x}) / \hat{q}_{\tau+1}(\mathbf{x}) \geq \tau + \gamma + d$. The desirable result then follows. \blacksquare

C.3 Proof of Lemma 3

Proof Without loss of generality, assume $\mathcal{L}(\varepsilon) \subset \{0, \dots, d-1\}$. Denote $l_L = \lfloor \hat{\sigma}(\mathbf{x})\Psi^{-1}(\varepsilon) + \hat{\mu}(\mathbf{x}) \rfloor - 1$ and $l_U = \lceil -\hat{\sigma}(\mathbf{x})\Psi^{-1}(\varepsilon) + \hat{\mu}(\mathbf{x}) \rceil$, $\xi_l = \mathbb{P}(\hat{\Gamma}(\mathbf{x}) = l)$, $\tilde{\xi}_l = \tilde{\mathbb{P}}(\hat{\Gamma}(\mathbf{x}) = l)$, $\xi_{-j,l} = \mathbb{P}(\hat{\Gamma}_{-j}(\mathbf{x}) = l)$, $\tilde{\xi}_{-j,l} = \tilde{\mathbb{P}}(\hat{\Gamma}_{-j}(\mathbf{x}) = l)$, we treat $|\tilde{\omega}_\tau - \bar{\omega}_\tau|$ and $|\tilde{v}_\tau - \bar{v}_\tau|$ separately. First,

$$\begin{aligned}
 |\tilde{\omega}_\tau - \bar{\omega}_\tau| &\leq \sum_{l > l_U} \frac{2}{\tau + l + \gamma + 1} \omega_{\tau,l} + \sum_{0 \leq l < l_L} \frac{2}{\tau + l + \gamma + 1} \omega_{\tau,l} + \sum_{l_L \leq l < l_U} \frac{2}{\tau + l + \gamma + 1} |\omega_{\tau,l} - \tilde{\omega}_{\tau,l}| \\
 &=: S_1 + S_2 + S_3.
 \end{aligned}$$

Next, we turn to bound S_1 - S_3 separately.

$$\begin{aligned}
 S_1 &= \sum_{l > l_U} \frac{2}{\tau + l + \gamma + 1} \sum_{s=1}^{\tau} \hat{q}_{j_s}(\mathbf{x}) \mathbb{P}(\hat{\Gamma}_{-j_s}(\mathbf{x}) = l) \leq \frac{2}{\tau + l_U + \gamma + 1} \sum_{s=1}^{\tau} \sum_{l > l_U} \mathbb{P}(\hat{\Gamma}_{-j_s}(\mathbf{x}) = l) \\
 &\leq \frac{2}{\tau + l_U + \gamma + 1} \sum_{s=1}^{\tau} (1 - \mathbb{P}(\hat{\Gamma}_{-j_s}(\mathbf{x}) \leq l_U)) \leq \frac{2\tau}{\tau + l_U + \gamma + 1} \mathbb{P}(\hat{\Gamma}(\mathbf{x}) > l_U),
 \end{aligned}$$

where the last inequality follows from Lemma 13. For S_2 , we have

$$S_2 \leq \frac{2}{\tau + \gamma + 1} \sum_{s=1}^{\tau} \sum_{0 \leq l < l_L} \mathbb{P}(\hat{\Gamma}_{-j_s}(\mathbf{x}) = l) \leq \frac{2\tau}{\tau + \gamma + 1} \mathbb{P}(\hat{\Gamma}(\mathbf{x}) \leq l_L + 1),$$

where the last inequality follows from Lemma 13. Next, according to Theorem 1.1 in Neammanee (2005),

$$\mathbb{P}(\hat{\Gamma}(\mathbf{x}) \leq l_L + 1) \leq \mathbb{P}(Z \leq \Psi^{-1}(\varepsilon)) + \frac{C_0}{\hat{\sigma}^2(\mathbf{x})} = \varepsilon + \frac{C_0}{\hat{\sigma}^2(\mathbf{x})},$$

and

$$\mathbb{P}(\hat{\Gamma}(\mathbf{x}) > l_U) \leq \mathbb{P}(Z \geq \Psi^{-1}(1 - \varepsilon)) + \frac{C_0}{\hat{\sigma}^2(\mathbf{x})} = \varepsilon + \frac{C_0}{\hat{\sigma}^2(\mathbf{x})},$$

where Z is a random variable following the refined normal distribution. For S_3 ,

$$\begin{aligned}
 S_3 &\leq \sum_{l=0}^{d-1} \frac{2}{\tau+l+\gamma+1} \sum_{s=1}^{\tau} \widehat{\mathbf{q}}_{js}(\mathbf{x}) |\widetilde{\xi}_{-j,l} - \xi_{-j,l}| \leq \sum_{s=1}^{\tau} \widehat{\mathbf{q}}_{js}(\mathbf{x}) \sum_{l=0}^{d-1} \frac{2}{\tau+l+\gamma+1} \max_{j=1,\dots,\tau} |\widetilde{\xi}_{-j,l} - \xi_{-j,l}| \\
 &\leq \min(\widehat{\mu}(\mathbf{x}), \tau) \sum_{l=0}^{d-1} \frac{2}{\tau+l+\gamma+1} \max_{s=1,\dots,\tau} \frac{C_0}{\widehat{\sigma}^2(\mathbf{x}) - \widehat{q}_{js}(\mathbf{x})(1 - \widehat{q}_{js}(\mathbf{x}))} \\
 &\leq \frac{2C_0 \min(\widehat{\mu}(\mathbf{x}), \tau)}{\widehat{\sigma}^2(\mathbf{x}) - 1/4} \sum_{l=1}^d \frac{1}{\tau+l+\gamma} = \frac{2C_0 \min(\widehat{\mu}(\mathbf{x}), \tau)}{\widehat{\sigma}^2(\mathbf{x}) - 1/4} (H_{\tau+d+\gamma} - H_{\tau+\gamma}) \\
 &\leq \frac{2C_0 \min(\widehat{\mu}(\mathbf{x}), \tau)}{\widehat{\sigma}^2(\mathbf{x}) - 1/4} \left(\log\left(1 + \frac{d}{\tau+\gamma}\right) + 1 - \frac{1}{\tau+\gamma} \right),
 \end{aligned}$$

where $H_K = \sum_{k=1}^K 1/k$ is the harmonic number, and the last inequality follows from the fact that $\log(K) + 1/K \leq H_K \leq \log(K) + 1$. Taken together,

$$|\widetilde{\omega}_\tau - \bar{\omega}_\tau| \leq \frac{4\tau}{\tau+\gamma+1} \left(\varepsilon + \frac{C_0}{\widehat{\sigma}^2(\mathbf{x})} \right) + \frac{2C_0 \min(\widehat{\mu}(\mathbf{x}), \tau)}{\widehat{\sigma}^2(\mathbf{x}) - 1/4} \left(\log\left(1 + \frac{d}{\tau+\gamma}\right) + \frac{\tau+\gamma-1}{\tau+\gamma} \right).$$

Similarly, for $|\widetilde{v}_\tau - \bar{v}_\tau|$,

$$|\widetilde{v}_\tau - \bar{v}_\tau| \leq \frac{2\gamma}{\tau+\gamma} \varepsilon + \frac{\gamma C_0}{\widehat{\sigma}^2(\mathbf{x})} \left(\log\left(1 + \frac{d}{\tau+\gamma-1}\right) + 1 - \frac{1}{\tau+\gamma-1} \right).$$

This completes the proof. ■

C.4 Proof of Lemma 4

Proof With the same argument in the proof of Lemma 3, it suffices to consider

$$|\widetilde{\mathbb{P}}(\widehat{\Gamma}(\mathbf{x}) = l) - \widetilde{\mathbb{P}}(\widehat{\Gamma}_{-j}(\mathbf{x}) = l)| \leq \sum_{l'=l-1}^l |\widetilde{\mathbb{P}}(\widehat{\Gamma}(\mathbf{x}) \leq l') - \widetilde{\mathbb{P}}(\widehat{\Gamma}_{-j}(\mathbf{x}) \leq l')|.$$

Denote $I = \widehat{\sigma}(\mathbf{x})^{-1}(l + 1/2 - \widehat{\mu}(\mathbf{x}))$ and $I_{-j} = \widehat{\sigma}_{-j}(\mathbf{x})^{-1}(l + 1/2 - \widehat{\mu}_{-j}(\mathbf{x}))$, we have

$$\begin{aligned}
 |\widetilde{\mathbb{P}}(\widehat{\Gamma}(\mathbf{x}) \leq l) - \widetilde{\mathbb{P}}(\widehat{\Gamma}_{-j}(\mathbf{x}) \leq l)| &= |\Psi(I) - \Psi_{-j}(I_{-j})| \\
 &\leq |\Phi(I) - \Phi(I_{-j})| + \frac{1}{6} |\widehat{\eta}(\mathbf{x})(1 - I^2)\phi(I) - \widehat{\eta}_{-j}(\mathbf{x})(1 - I_{-j}^2)\phi(I_{-j})| =: T_1 + \frac{1}{6}T_2.
 \end{aligned}$$

Next, we turn to treat T_1 and T_2 separately. Without loss generalization, we assume $|I_{-j}| \geq |I|$, then

$$\begin{aligned}
 T_1 &\leq \left| \int_I^{I_{-j}} \phi(\mathbf{x}) d\mathbf{x} \right| \leq |I_{-j} - I| \phi(I) \\
 &= \left(|\widehat{\sigma}^{-1}(\mathbf{x}) - \widehat{\sigma}_{-j}^{-1}(\mathbf{x})| |l + 1/2 - \widehat{\mu}(\mathbf{x})| + \widehat{\sigma}_{-j}^{-1}(\mathbf{x}) |\widehat{\mu}(\mathbf{x}) - \widehat{\mu}_{-j}(\mathbf{x})| \right) \phi(I) \\
 &= \widehat{\sigma}_{-j}^{-1}(\mathbf{x}) (\widehat{\sigma}(\mathbf{x}) - \widehat{\sigma}_{-j}(\mathbf{x})) |I| \phi(I) + \widehat{\sigma}_{-j}^{-1}(\mathbf{x}) \widehat{q}_j(\mathbf{x}) \phi(I) \\
 &\leq \frac{\widehat{q}_j(\mathbf{x})(1 - \widehat{q}_j(\mathbf{x}))}{\widehat{\sigma}_{-j}(\mathbf{x})(\widehat{\sigma}_{-j}(\mathbf{x}) + \widehat{\sigma}(\mathbf{x}))} |I| \phi(I) + \frac{1}{\sqrt{2\pi} \widehat{\sigma}_{-j}(\mathbf{x})} \leq \frac{1}{4\sqrt{2\pi}} \left(\frac{1}{2\sqrt{e}(\widehat{\sigma}^2(\mathbf{x}) - 1/4)} + \frac{4}{\sqrt{\widehat{\sigma}^2(\mathbf{x}) - 1/4}} \right),
 \end{aligned}$$

where the last inequality follows the fact that $|u|\phi(u) \leq 1/\sqrt{2e\pi}$ and $0 \leq \phi(u) \leq 1/\sqrt{2\pi}$. For T_2 , let $g(u) = (1 - u^2)\phi(u)$, we have

$$T_2 \leq |\hat{\eta}(\mathbf{x})(1 - I^2)\phi(I)| + |\hat{\eta}_{-j}(\mathbf{x})(1 - I_{-j}^2)\phi(I_{-j})| \leq \frac{1}{\sqrt{2\pi}} \frac{\hat{m}_3(\mathbf{x})}{(\hat{\sigma}^2(\mathbf{x}) - 1/4)^{3/2}},$$

where the last inequality follows from the fact that $|g(u)| \leq 1/\sqrt{2\pi}$, and $\hat{m}_3(\mathbf{x}) = \sum_{j=1}^d \hat{p}_j(\mathbf{x})(1 - \hat{p}_j(\mathbf{x}))(1 - 2\hat{p}_j(\mathbf{x}))$. Taken together, using the same argument in the proof of Lemma 3, we have

$$|\tilde{\omega}_\tau^b - \tilde{\omega}_\tau| \leq \frac{1}{4\sqrt{2\pi}} \left(\frac{1/(2\sqrt{e})}{\hat{\sigma}^2(\mathbf{x}) - 1/4} + \frac{4}{\sqrt{\hat{\sigma}^2(\mathbf{x}) - 1/4}} + \frac{4\hat{m}_3(\mathbf{x})}{(\hat{\sigma}^2(\mathbf{x}) - 1/4)^{3/2}} \right) \left(\log \left(1 + \frac{d}{\tau + \gamma} \right) + 1 \right).$$

Combining Lemma 3, the desirable result then follows. \blacksquare

C.5 Proof of Lemma 5

Proof Denote $\mathcal{K}_+ = \{1 \leq k \leq K : \alpha_k > 0\}$. We first prove the necessity. Suppose Δ_k^* is a global minimizer of $\text{Dice}_k(\cdot)$, for $k \in \mathcal{K}_+$. Then for any $\Delta = (\Delta_1, \dots, \Delta_K)$, we have

$$\text{mDice}_\gamma(\Delta^*) = \sum_{k \in \mathcal{K}_+} \alpha_k \text{Dice}_{\gamma,k}(\Delta_k^*) \leq \sum_{k \in \mathcal{K}_+} \alpha_k \text{Dice}_{\gamma,k}(\Delta_k),$$

yields that Δ^* is a global minimizer of $\text{mDice}_\gamma(\cdot)$. We next prove the sufficiency by contradiction. Suppose Δ^* is a global minimizer of $\text{mDice}_\gamma(\cdot)$, yet there exists $k_0 \in \mathcal{K}_+$ such that $\Delta_{k_0}^*$ is not a minimizer of $\text{Dice}_{\gamma,k_0}(\cdot)$. Thus, there exists a segmentation rule $\tilde{\Delta}$ such that $\text{Dice}_{\gamma,k_0}(\tilde{\Delta}) < \text{Dice}_{\gamma,k_0}(\Delta_{k_0}^*)$, then let $\tilde{\Delta} = (\Delta_1^*, \dots, \Delta_{k_0-1}^*, \tilde{\Delta}_{k_0}, \Delta_{k_0+1}^*, \dots, \Delta_K^*)$

$$\text{mDice}_\gamma(\Delta^*) = \sum_{k \in \mathcal{K}_+} \alpha_k \text{Dice}_{\gamma,k}(\Delta_k^*) > \sum_{k \in \mathcal{K}_+} \alpha_k \text{Dice}_{\gamma,k}(\tilde{\Delta}) = \text{mDice}_\gamma(\tilde{\Delta}),$$

which leads to contradiction of that Δ^* is a global minimizer of $\text{mDice}_\gamma(\cdot)$. The desirable result then follows. \blacksquare

C.6 Proof of Lemma 6

Proof Given a segmentation rule $\Delta(\mathbf{X}) = (\Delta_1(\mathbf{X}), \dots, \Delta_K(\mathbf{X}))$, $\text{mDice}_\gamma(\cdot)$ can be rewritten as

$$\text{mDice}_\gamma(\Delta) = \sum_{k=1}^K \alpha_k \text{Dice}_{\gamma,k}(\Delta_k(\mathbf{X})).$$

It is equivalent to consider the point-wise minimization on $\mathbf{X} = \mathbf{x}$:

$$\Delta^*(\mathbf{x}) = \underset{\mathbf{V} \in \{0,1\}^{d \times K}}{\text{argmax}} \text{mDice}_\gamma(\mathbf{V}|\mathbf{x}), \quad \text{s.t.} \sum_{k=1}^K \mathbf{V}_k = \mathbf{1}_d, \quad \text{mDice}_\gamma(\mathbf{V}|\mathbf{x}) = \sum_{k=1}^K \alpha_k \text{Dice}_{\gamma,k}(\mathbf{V}_k|\mathbf{x}),$$

where \mathbf{V}_k is the k -th column of \mathbf{V} . According to (25), we have

$$\begin{aligned} \text{mDice}_\gamma(\mathbf{V}|\mathbf{x}) &= \sum_{k=1}^K \alpha_k \sum_{j \in I(\mathbf{V}_k)} \sum_{\substack{\mathbf{y}_{-j,k} \in \{0,1\}^{d-1} \\ y_{j,k}=1}} \frac{2\mathbb{P}(\mathbf{Y}_k = \mathbf{y}_k|\mathbf{x})}{\tau_k + \|\mathbf{y}_k\|_1 + \gamma} + \sum_{k=1}^K \alpha_k \mathbb{E}\left(\frac{\gamma}{\|\mathbf{Y}_{\cdot k}\|_1 + \tau_k + \gamma}\right) \\ &= \sum_{k=1}^K \sum_{j=1}^d R_{jk}(\tau_k) v_{jk} + \sum_{k=1}^K \alpha_k \bar{v}(\tau_k), \end{aligned}$$

where $v_{jk} \in \{0, 1\}$ is the segmentation indicator of the j -th feature under the class- k , and $R_{jk}(\cdot)$ is a reward function defined as:

$$R_{jk}(\tau_k) = \alpha_k \sum_{\substack{\mathbf{y}_{-j,k} \in \{0,1\}^{d-1} \\ y_{j,k}=1}} \frac{2\mathbb{P}(\mathbf{Y}_k = \mathbf{y}_k|\mathbf{x})}{\tau_k + \|\mathbf{y}_k\|_1}.$$

Now, suppose the optimal volume function $\boldsymbol{\tau}^*(\mathbf{x}) = (\tau_1^*(\mathbf{x}), \dots, \tau_K^*(\mathbf{x}))^\top$ is given, then $\bar{v}(\tau_k^*)$ becomes a constant, and the point-wise maximization on mDice_γ is equivalent to:

$$\begin{aligned} &\max_{\mathbf{v} \in \{0,1\}^{d \times K}} \sum_{k=1}^K \sum_{j=1}^d R_{jk}^* v_{jk}, \\ &\text{subject to } \sum_{j=1}^d v_{jk} = \tau_k^*(\mathbf{x}), \quad \sum_{k=1}^K v_{jk} = 1, \quad \text{for } k = 1, \dots, K; \quad \text{for } j = 1, \dots, d, \end{aligned} \quad (28)$$

where $R_{jk}^* = R_{jk}(\tau_k^*(\mathbf{x}))$ is the reward under $\tau_k^*(\mathbf{x})$. Note that (28) is the formulation for the assignment problem (Kuhn, 1955). This completes the proof. \blacksquare

C.7 Proof of Lemma 8

Proof For simplicity, we construct a counter example based on $\gamma = 0$ and $d = 2$, that is, $\mathbf{Y} = (Y_1, Y_2)^\top$ and $\mathbf{q}(\mathbf{x}) = (q_1(\mathbf{x}), q_2(\mathbf{x}))^\top$. Without loss generality, we assume $p_1(\mathbf{x}) > p_2(\mathbf{x})$.

First, we derive the Bayes rule in Theorem 1 for this case. Note that it suffices to compare the scores for $\tau = 1$ ($\mathbf{v} = (1, 0)^\top$) and $\tau = 2$ ($\mathbf{v} = (1, 1)^\top$).

$$\text{Dice}((1, 0)^\top|\mathbf{x}) = p_1(\mathbf{x}) + \frac{1}{3}p_1(\mathbf{x})p_2(\mathbf{x}), \quad \text{Dice}((1, 1)^\top|\mathbf{x}) = \frac{2}{3}(p_1(\mathbf{x}) + p_2(\mathbf{x})) - \frac{1}{3}p_1(\mathbf{x})p_2(\mathbf{x}).$$

Therefore, the Bayes rule for Dice optimal segmentation is:

$$\boldsymbol{\delta}^*(\mathbf{x}) = (1, 0)^\top, \text{ if } \frac{1}{2}p_1(\mathbf{x}) - p_2(\mathbf{x}) + p_1(\mathbf{x})p_2(\mathbf{x}) \geq 0, \quad \boldsymbol{\delta}^*(\mathbf{x}) = (1, 1)^\top, \text{ otherwise.}$$

Now, we check the Dice-calibrated (Fisher consistency) for classification-calibrated losses (CCL). Let $p_1(\mathbf{x}) = 0.45$ and $p_2(\mathbf{x}) = 0.44$, then $\tilde{\boldsymbol{\delta}}(\mathbf{x}) = \mathbf{1}(\mathbf{p}(\mathbf{x}) \geq 0.5) = (0, 0)^\top \neq (1, 1)^\top = \boldsymbol{\delta}^*(\mathbf{x})$, where the first equality follows from the definition of a classification-calibrated loss. Therefore, $\text{Dice}(\tilde{\boldsymbol{\delta}}) < \text{Dice}(\boldsymbol{\delta}^*)$ yields that a classification-calibrated loss with thresholding at 0.5 is not Dice-calibrated.

Next, we check the Dice calibration for soft-Dice loss. Again, it suffices to consider the point-wise minimization given $\mathbf{X} = \mathbf{x}$, and its gradients with respect to $c_j = q_j(\mathbf{x}) \in [0, 1]$ for $j = 1, 2$:

$$\begin{aligned} \frac{\partial \mathbb{E}(l_{\text{SoftD}}(\mathbf{Y}, \mathbf{c}) \mid \mathbf{X} = \mathbf{x})}{\partial c_1} &= -2\mathbb{E}\left(\frac{Y_1(Y_1 + Y_2 + c_1 + c_2) - (Y_1 c_1 + Y_2 c_2)}{(Y_1 + Y_2 + c_1 + c_2)^2} \mid \mathbf{X} = \mathbf{x}\right) \\ &= -2\left(\frac{2p_1(\mathbf{x})p_1(\mathbf{x})}{(2 + c_1 + c_2)^2} + \frac{p_1(\mathbf{x})(1 - p_2(\mathbf{x})) + (p_1(\mathbf{x}) - p_2(\mathbf{x}))c_2}{(1 + c_1 + c_2)^2}\right), \\ \frac{\partial \mathbb{E}(l_{\text{SoftD}}(\mathbf{Y}, \mathbf{c}) \mid \mathbf{X} = \mathbf{x})}{\partial c_2} &= -2\left(\frac{2p_1(\mathbf{x})p_1(\mathbf{x})}{(2 + c_1 + c_2)^2} + \frac{p_2(\mathbf{x})(1 - p_1(\mathbf{x})) + (p_2(\mathbf{x}) - p_1(\mathbf{x}))c_1}{(1 + c_1 + c_2)^2}\right). \end{aligned}$$

Accordingly, $\partial \mathbb{E}(l_{\text{SoftD}}(\mathbf{Y}, \mathbf{c}) \mid \mathbf{X} = \mathbf{x}) / \partial c_1 \leq 0$ for any $c_2 \in [0, 1]$, and $\partial \mathbb{E}(l_{\text{SoftD}}(\mathbf{Y}, \mathbf{c}) \mid \mathbf{X} = \mathbf{x}) / \partial c_2 \leq 0$ when $2p_2(\mathbf{x}) - p_1(\mathbf{x}) - p_1(\mathbf{x})p_2(\mathbf{x}) \geq 0$. For example, let $p_1(\mathbf{x}) = 0.45$ and $p_2(\mathbf{x}) = 0.4$, then $\tilde{\boldsymbol{\delta}}(\mathbf{x}) = (1, 1)^\top \neq (1, 0)^\top = \boldsymbol{\delta}^*(\mathbf{x})$. Therefore, $\text{Dice}(\tilde{\boldsymbol{\delta}}) < \text{Dice}(\boldsymbol{\delta}^*)$ yields that the soft-Dice loss with thresholding at 0.5 is not Dice-calibrated. This completes the proof. \blacksquare

C.8 Proof of Lemma 9

Proof By the definition of a strictly proper loss and the formulation in (24), we have $\hat{\mathbf{q}}(\mathbf{x}) = \mathbf{p}(\mathbf{x}) = (\mathbb{P}(Y_1 = 1 \mid \mathbf{X} = \mathbf{x}), \dots, \mathbb{P}(Y_d = 1 \mid \mathbf{X} = \mathbf{x}))^\top$. Then the estimation of $\hat{\boldsymbol{\tau}}(\mathbf{x})$ and $\hat{\boldsymbol{\delta}}(\mathbf{x})$ agrees with the definition of $\boldsymbol{\tau}^*(\mathbf{x})$ and $\boldsymbol{\delta}^*(\mathbf{x})$. This completes the proof. \blacksquare

C.9 Proof of Theorem 10

Proof First, we consider point-wise approximation of the Dice metric under probabilities \mathbf{p} and $\hat{\mathbf{q}}$. For any $\boldsymbol{\delta}$, such that $\delta_j(\mathbf{x}) = 1$ for $j = j_1, \dots, j_\tau$, and $\delta_j(\mathbf{x}) = 0$ otherwise. Define

$$\begin{aligned} \widehat{\text{Dice}}_\gamma(\boldsymbol{\delta}(\mathbf{x}) \mid \mathbf{X} = \mathbf{x}) &:= \sum_{s=1}^{\tau} \sum_{l=0}^{d-1} \frac{2\hat{q}_{j_s}(\mathbf{x})\mathbb{P}(\hat{\Gamma}_{-j}(\mathbf{x}) = l)}{\tau + l + \gamma + 1} + \sum_{l=0}^d \frac{\gamma\mathbb{P}(\hat{\Gamma}(\mathbf{X}) = l)}{\tau + l + \gamma} \\ &= \sum_{s=1}^{\tau} 2\hat{q}_{j_s}(\mathbf{x})\mathbb{E}\left(\frac{1}{\tau + \gamma + 1 + \hat{\Gamma}_{-j_s}(\mathbf{x})}\right) + \gamma\mathbb{E}\left(\frac{1}{\tau + \gamma + \hat{\Gamma}(\mathbf{x})}\right) \\ \text{Dice}_\gamma(\boldsymbol{\delta}(\mathbf{x}) \mid \mathbf{X} = \mathbf{x}) &:= \sum_{s=1}^{\tau} \sum_{l=0}^{d-1} \frac{2p_{j_s}(\mathbf{x})\mathbb{P}(\Gamma_{-j}(\mathbf{x}) = l)}{\tau + l + \gamma + 1} + \sum_{l=0}^d \frac{\gamma\mathbb{P}(\Gamma(\mathbf{X}) = l)}{\tau + l + \gamma} \\ &= \sum_{s=1}^{\tau} 2p_{j_s}(\mathbf{x})\mathbb{E}\left(\frac{1}{\tau + \gamma + 1 + \Gamma_{-j_s}(\mathbf{x})}\right) + \gamma\mathbb{E}\left(\frac{1}{\tau + \gamma + \Gamma(\mathbf{x})}\right). \end{aligned}$$

Now, we have

$$\begin{aligned}
 & \left| \widehat{\text{Dice}}_\gamma(\boldsymbol{\delta}(\mathbf{x})|\mathbf{X}=\mathbf{x}) - \text{Dice}_\gamma(\boldsymbol{\delta}(\mathbf{x})|\mathbf{X}=\mathbf{x}) \right| \\
 & \leq \left| 2 \sum_{s=1}^{\tau} \left(\widehat{q}_{j_s}(\mathbf{x}) \mathbb{E} \left(\frac{1}{\tau + \gamma + 1 + \widehat{\Gamma}_{-j_s}(\mathbf{x})} \right) - p_{j_s}(\mathbf{x}) \mathbb{E} \left(\frac{1}{\tau + \gamma + 1 + \Gamma_{-j_s}(\mathbf{x})} \right) \right) \right. \\
 & \quad \left. + \gamma \left| \mathbb{E} \left(\frac{1}{\tau + \gamma + \widehat{\Gamma}(\mathbf{x})} \right) - \mathbb{E} \left(\frac{1}{\tau + \gamma + \Gamma(\mathbf{x})} \right) \right| \right| \\
 & \leq \left| 2 \sum_{s=1}^{\tau} \widehat{q}_{j_s}(\mathbf{x}) \left(\mathbb{E} \left(\frac{1}{\tau + \gamma + 1 + \widehat{\Gamma}_{-j_s}(\mathbf{x})} \right) - \mathbb{E} \left(\frac{1}{\tau + \gamma + 1 + \Gamma_{-j_s}(\mathbf{x})} \right) \right) \right| \\
 & \quad + \left| 2 \sum_{s=1}^{\tau} (\widehat{q}_{j_s}(\mathbf{x}) - p_{j_s}(\mathbf{x})) \mathbb{E} \left(\frac{1}{\tau + \gamma + 1 + \Gamma_{-j_s}(\mathbf{x})} \right) \right| + \gamma \left| \mathbb{E} \left(\frac{1}{\tau + \gamma + \widehat{\Gamma}(\mathbf{x})} \right) - \mathbb{E} \left(\frac{1}{\tau + \gamma + \Gamma(\mathbf{x})} \right) \right| \\
 & \leq 2 \sum_{s=1}^{\tau} \left| \frac{\mathbb{E}(\Gamma_{-j_s}(\mathbf{x}) - \widehat{\Gamma}_{-j_s}(\mathbf{x}))}{(\tau + \gamma + 1)^2} \right| + 2 \sum_{s=1}^{\tau} \frac{|\widehat{q}_{j_s}(\mathbf{x}) - p_{j_s}(\mathbf{x})|}{\tau + \gamma + 1} + \gamma \left| \frac{\mathbb{E}(\Gamma(\mathbf{x}) - \widehat{\Gamma}(\mathbf{x}))}{(\tau + \gamma)^2} \right| \\
 & \leq 2 \sum_{s=1}^{\tau} \frac{\|\widehat{\mathbf{q}}(\mathbf{x})\|_1 - \|\mathbf{p}(\mathbf{x})\|_1 + |\widehat{q}_{j_s}(\mathbf{x}) - p_{j_s}(\mathbf{x})|}{(\tau + \gamma + 1)^2} + 2 \sum_{s=1}^{\tau} \frac{|\widehat{q}_{j_s}(\mathbf{x}) - p_{j_s}(\mathbf{x})|}{\tau + \gamma + 1} + \gamma \frac{\|\widehat{\mathbf{q}}(\mathbf{x})\|_1 - \|\mathbf{p}(\mathbf{x})\|_1}{(\tau + \gamma)^2} \\
 & \leq \left(\frac{3}{2(1 + \gamma)} + c_1 \right) \|\widehat{\mathbf{q}}(\mathbf{x}) - \mathbf{p}(\mathbf{x})\|_1,
 \end{aligned}$$

where the second inequality follows from the triangle inequality, $c_1 = 0$ if $\gamma = 0$, $c_1 = 1/\gamma$ if $\gamma > 0$. Therefore,

$$\begin{aligned}
 \text{Dice}_\gamma(\boldsymbol{\delta}^*) - \text{Dice}_\gamma(\widehat{\boldsymbol{\delta}}) &= \text{Dice}_\gamma(\boldsymbol{\delta}^*) - \widehat{\text{Dice}}_\gamma(\boldsymbol{\delta}^*) + \widehat{\text{Dice}}_\gamma(\boldsymbol{\delta}^*) - \widehat{\text{Dice}}_\gamma(\widehat{\boldsymbol{\delta}}) + \widehat{\text{Dice}}_\gamma(\widehat{\boldsymbol{\delta}}) - \text{Dice}_\gamma(\widehat{\boldsymbol{\delta}}) \\
 &\leq \text{Dice}_\gamma(\boldsymbol{\delta}^*) - \widehat{\text{Dice}}_\gamma(\boldsymbol{\delta}^*) + \widehat{\text{Dice}}_\gamma(\widehat{\boldsymbol{\delta}}) - \text{Dice}_\gamma(\widehat{\boldsymbol{\delta}}) \\
 &\leq \mathbb{E}_{\mathbf{X}} \left| \widehat{\text{Dice}}_\gamma(\boldsymbol{\delta}^*(\mathbf{X})|\mathbf{X}) - \text{Dice}_\gamma(\boldsymbol{\delta}^*(\mathbf{X})|\mathbf{X}) \right| + \mathbb{E}_{\mathbf{X}} \left| \widehat{\text{Dice}}_\gamma(\widehat{\boldsymbol{\delta}}(\mathbf{X})|\mathbf{X}) - \text{Dice}_\gamma(\widehat{\boldsymbol{\delta}}(\mathbf{X})|\mathbf{X}) \right| \\
 &\leq \left(\frac{3}{1 + \gamma} + 2c_1 \right) \mathbb{E} \|\widehat{\mathbf{q}}(\mathbf{X}) - \mathbf{p}(\mathbf{X})\|_1,
 \end{aligned}$$

where the first inequality follows from the definition of $\widehat{\boldsymbol{\delta}}$ such that $\widehat{\text{Dice}}_\gamma(\boldsymbol{\delta}^*) - \widehat{\text{Dice}}_\gamma(\widehat{\boldsymbol{\delta}}) \leq 0$. This completes the proof. \blacksquare

Proof of Corollary 11

Proof According to the Pinsker's inequality, we have

$$\begin{aligned}
 \mathbb{E}_{\mathbf{X}} \|\widehat{\mathbf{q}}(\mathbf{X}) - \mathbf{p}(\mathbf{X})\|_1 &= \sum_{j=1}^d \mathbb{E}_{\mathbf{X}} |\widehat{q}_j(\mathbf{X}) - p_j(\mathbf{X})| \leq \sum_{j=1}^d \mathbb{E}_{\mathbf{X}} \sqrt{\frac{1}{2} \text{KL}(\mathbb{P}(Y_j|\mathbf{X}), \widehat{\mathbb{P}}(Y_j|\mathbf{X}))} \\
 &\leq \sqrt{\frac{d}{2} \sum_{j=1}^d \mathbb{E}_{\mathbf{X}} \text{KL}(\mathbb{P}(Y_j|\mathbf{X}), \widehat{\mathbb{P}}(Y_j|\mathbf{X}))} = \sqrt{\frac{d}{2}} \sqrt{\mathbb{E} \left(l_{\text{CE}}(\mathbf{Y}, \widehat{\mathbf{q}}(\mathbf{X})) \right) - \mathbb{E} \left(l_{\text{CE}}(\mathbf{Y}, \mathbf{p}(\mathbf{X})) \right)},
 \end{aligned}$$

where the last inequality follows from the Cauchy-Schwarz inequality and the Jensen's inequality, and $\text{KL}(\mathbb{P}(Y_j|\mathbf{x}), \widehat{\mathbb{P}}(Y_j|\mathbf{x})) := p_j(\mathbf{x}) \log(p_j(\mathbf{x})/\widehat{q}_j(\mathbf{x})) + (1 - p_j(\mathbf{x})) \log((1 - p_j(\mathbf{x}))/(1 - \widehat{q}_j(\mathbf{x})))$ is

the KL divergence between $\mathbb{P}(Y_j|\mathbf{x})$ under \mathbf{p} and $\hat{\mathbb{P}}(Y_j|\mathbf{x})$ under $\hat{\mathbf{q}}$. The desirable result then follows by combining (19) in Theorem 10. This completes the proof. \blacksquare

C.10 Proof of Lemma 12

Proof Denote $\mathbf{y}_I = (y_j : j \in I)^\top$, $\mathbf{y}_{-I} = (y_j : j \notin I)^\top$, and let $I(\mathbf{v}) = I(\boldsymbol{\delta}(\mathbf{x})) = \{j : v_j = 1\}$ be a segmentation index set, and $\|\mathbf{v}\|_1 = \tau$. Again, consider the point-wise maximization:

$$\boldsymbol{\delta}^*(\mathbf{x}) = \operatorname{argmax}_{\mathbf{v} \in \{0,1\}^d} \operatorname{IoU}_\gamma(\mathbf{v}|\mathbf{x}),$$

where $\operatorname{IoU}_\gamma(\mathbf{v}|\mathbf{x})$ is defined as

$$\begin{aligned} \operatorname{IoU}_\gamma(\mathbf{v}|\mathbf{x}) &= \mathbb{E} \left(\frac{\|\mathbf{Y}_{I(\mathbf{v})}\|_1 + \gamma}{\|\mathbf{Y}_{-I(\mathbf{v})}\|_1 + \|\mathbf{v}\|_1 + \gamma} \middle| \mathbf{X} = \mathbf{x} \right) \\ &= \mathbb{E} \left(\frac{\|\mathbf{Y}_{I(\mathbf{v})}\|_1}{\|\mathbf{Y}_{-I(\mathbf{v})}\|_1 + \tau + \gamma} \middle| \mathbf{X} = \mathbf{x} \right) + \mathbb{E} \left(\frac{\gamma}{\|\mathbf{Y}_{-I(\mathbf{v})}\|_1 + \tau + \gamma} \middle| \mathbf{X} = \mathbf{x} \right) \\ &= \left(\mathbb{E}(\|\mathbf{Y}_{I(\mathbf{v})}\|_1 | \mathbf{X} = \mathbf{x}) + \gamma \right) \mathbb{E} \left(\frac{1}{\|\mathbf{Y}_{-I(\mathbf{v})}\|_1 + \tau + \gamma} \middle| \mathbf{X} = \mathbf{x} \right), \end{aligned}$$

where the last equality follows from the fact that $\mathbf{Y}_{I(\mathbf{v})} \perp \mathbf{Y}_{-I(\mathbf{v})} | \mathbf{X}$. Fix $\tau = \|\mathbf{v}\|_1$. The first term is maximized at $\mathbf{v}^* = (v_1^*, \dots, v_d^*)$ with

$$v_j^* = \begin{cases} 1 & \text{if } p_j(\mathbf{x}) \text{ ranks top } \tau, \\ 0 & \text{otherwise,} \end{cases}$$

and the maximum value is $\sum_{j \in J_\tau(\mathbf{x})} p_j(\mathbf{x}) + \gamma$. The second term is

$$\mathbb{E} \left(\frac{1}{\|\mathbf{Y}_{-I(\mathbf{v})}\|_1 + \tau + \gamma} \middle| \mathbf{X} = \mathbf{x} \right) = \mathbb{E} \left(\frac{1}{\Gamma_{-I(\mathbf{v})}(\mathbf{x}) + \tau + \gamma} \right).$$

Given $I(\mathbf{v}) \neq I(\mathbf{v}^*)$, we have $\Gamma_{-I(\mathbf{v})}(\mathbf{x}) = \sum_{j=1}^{d-\tau} B_j$ and $\Gamma_{-I(\mathbf{v}^*)}(\mathbf{x}) = \sum_{j=1}^{d-\tau} B_j^*$, where B_j and B_j^* are independent Bernoulli variables with success probability $p_j \geq p_j^*$, respectively, for $j = 1, \dots, d - \tau$. By Theorem 2.2.9 of Belzunce et al. (2015), $\Gamma_{-I(\mathbf{v})}(\mathbf{x})$ is stochastically greater than $\Gamma_{-I(\mathbf{v}^*)}(\mathbf{x})$, namely

$$\mathbb{P}(\Gamma_{-I(\mathbf{v})}(\mathbf{x}) \leq \varsigma) \leq \mathbb{P}(\Gamma_{-I(\mathbf{v}^*)}(\mathbf{x}) \leq \varsigma)$$

for any $\varsigma \in \mathbb{R}$. Thus,

$$\begin{aligned} \mathbb{E} \left(\frac{1}{\Gamma_{-I(\mathbf{v})}(\mathbf{x}) + \tau + \gamma} \right) &= \int_0^\infty \mathbb{P} \left(\frac{1}{\Gamma_{-I(\mathbf{v})}(\mathbf{x}) + \tau + \gamma} \geq \varsigma \right) d\varsigma \\ &\leq \int_0^\infty \mathbb{P} \left(\frac{1}{\Gamma_{-I(\mathbf{v}^*)}(\mathbf{x}) + \tau + \gamma} \geq \varsigma \right) d\varsigma = \mathbb{E} \left(\frac{1}{\Gamma_{-I(\mathbf{v}^*)}(\mathbf{x}) + \tau + \gamma} \right). \end{aligned}$$

As a result, the second term is also maximized at \mathbf{v}^* . Therefore, \mathbf{v}^* maximizes $\operatorname{IoU}_\gamma(\mathbf{v}|\mathbf{x})$ for a fixed τ . The desired result follows. \blacksquare

D. Auxiliary Lemmas

Lemma 13 Suppose $\Gamma = \sum_{j=1}^d B_j$ is a Poisson binomial random variable, and $B_j (j = 1, \dots, d)$ are independent Bernoulli trials with success probabilities p_1, \dots, p_d . Then, for any $j = 1, \dots, d$, we have

$$\mathbb{P}(\Gamma_{-j} \leq l-1) \leq \mathbb{P}(\Gamma \leq l) \leq \mathbb{P}(\Gamma_{-j} \leq l),$$

where $\Gamma_{-j} = \sum_{j' \neq j} B_{j'}$.

Proof Note that $\Gamma = \Gamma_{-j} + B_j$, then

$$\begin{aligned} \mathbb{P}(\Gamma \leq l) &= \mathbb{P}(\Gamma_{-j} + B_j \leq l) = \mathbb{P}(\Gamma_{-j} \leq l \mid B_j = 0)(1 - p_j) + \mathbb{P}(\Gamma_{-j} \leq l-1 \mid B_j = 1)p_j \\ &= \mathbb{P}(\Gamma_{-j} \leq l)(1 - p_j) + \mathbb{P}(\Gamma_{-j} \leq l-1)p_j, \end{aligned}$$

where the last equality follows from the fact that $B_j \perp B_{j'}$ for $j \neq j'$. The desirable result then follows since $\mathbb{P}(\Gamma_{-j} \leq l) \geq \mathbb{P}(\Gamma_{-j} \leq l-1)$. \blacksquare

Lemma 14 Suppose $\Gamma = \sum_{j=1}^d B_j$ is a Poisson binomial random variable, and $B_j (j = 1, \dots, d)$ are independent Bernoulli trials with success probabilities $p_1 \geq p_2 \geq \dots \geq p_d$. Then, for an arbitrary positive non-decreasing sequence $\zeta_l (l = 0, \dots, d-1)$,

$$Q_j = \sum_{l=0}^{d-1} \frac{1}{\zeta_l} \mathbb{P}(\Gamma_{-j} = l)$$

is a non-increasing function with respect to $j = 1, \dots, d$.

Proof Note that for any $j' \neq j$, $\Gamma_{-j} = \sum_{i \neq j} B_i = \sum_{i \neq j, j'} B_i + B_{j'} =: \Gamma_{-jj'} + B_{j'}$. Denote $\xi_{-jj', l} = \mathbb{P}(\Gamma_{-jj'} = l)$, we have

$$\mathbb{P}(\Gamma_{-j} = l) = (1 - p_{j'}) \xi_{-jj', l} + p_{j'} \xi_{-jj', l-1}.$$

Then,

$$\begin{aligned} Q_j - Q_{j'} &= \sum_{l=0}^d \frac{1}{\zeta_l} ((1 - p_{j'}) \xi_{-jj', l} + p_{j'} \xi_{-jj', l-1} - (1 - p_j) \xi_{-jj', l} - p_j \xi_{-jj', l-1}) \\ &= \sum_{l=0}^d \frac{1}{\zeta_l} (\xi_{-jj', l} - \xi_{-jj', l-1}) = (p_j - p_{j'}) \left(\sum_{l=0}^d \frac{1}{\zeta_l} \xi_{-jj', l} - \sum_{l=0}^d \frac{1}{\zeta_l} \xi_{-jj', l-1} \right) \\ &= (p_j - p_{j'}) \left(\sum_{l=0}^d \left(\frac{1}{\zeta_l} - \frac{1}{\zeta_{l+1}} \right) \xi_{-jj', l} \right), \end{aligned}$$

where the first equality follows from the fact that $\mathbb{P}(\Gamma_{-j} = d) = 0$, and the last equality follows from the fact that $\xi_{-jj', l} = 0$ for $l < 0$. Hence, we have $Q_j - Q_{j'}$ has the same sign with $p_j - p_{j'}$, and the desirable result then follows. \blacksquare

Lemma 15 *Let Γ be a Poisson-binomial random variable with the success probability $(p_j)_{j=1,\dots,d}$, then for any $\tau \geq 1$, we have*

$$(\sum_{j=1}^d p_j + \tau)^{-1} \leq \mathbb{E}\left(\frac{1}{\Gamma + \tau}\right) \leq \left(\frac{d+1}{d} \sum_{j=1}^d p_j + \tau - 1\right)^{-1}.$$

Proof According to the corollary in Chao and Strawderman (1972), we have

$$\begin{aligned} \mathbb{E}\left(\frac{1}{\Gamma + \tau}\right) &= \int_0^1 t^{\tau-1} P_\Gamma(t) dt = \int_0^1 t^{\tau-1} \left(\prod_{j=1}^d (1 - p_j + p_j t)\right) dt \leq \int_0^1 t^{\tau-1} (1 - \bar{p} + \bar{p}t)^d dt \\ &= \mathbb{E}\left(\frac{1}{\Lambda + \tau}\right) \leq \left(\frac{d+1}{d} \sum_{j=1}^d p_j + \tau - 1\right)^{-1}, \end{aligned}$$

where $\bar{p} = d^{-1} \sum_{j=1}^d p_j$, the first inequality follows from the inequality of arithmetic and geometric means, the last equality follows from Section 3.1 of Chao and Strawderman (1972), and the last inequality follows from (25) in Wooff (1985). This completes the proof. \blacksquare

References

- Miklós Ajtai, János Komlós, and Endre Szemerédi. An $O(n \log n)$ sorting network. In *Proceedings of the Fifteenth Annual ACM Symposium on Theory of Computing*, pages 1–9, 1983.
- Abdulhakam AM Assidiq, Othman O Khalifa, Md Rafiqul Islam, and Sheroz Khan. Real time lane detection for autonomous vehicles. In *2008 International Conference on Computer and Communication Engineering*, pages 82–88. IEEE, 2008.
- Vijay Badrinarayanan, Alex Kendall, and Roberto Cipolla. Segnet: A deep convolutional encoder-decoder architecture for image segmentation. *IEEE Transactions on Pattern Analysis and Machine Intelligence*, 39(12):2481–2495, 2017.
- Peter L Bartlett, Olivier Bousquet, and Shahar Mendelson. Local rademacher complexities. *Annals of Statistics*, 33(4):1497–1537, 2005.
- Peter L Bartlett, Michael I Jordan, and Jon D McAuliffe. Convexity, classification, and risk bounds. *Journal of the American Statistical Association*, 101(473):138–156, 2006.
- Felix Belzunce, Carolina Martinez Riquelme, and Julio Mulero. *An introduction to stochastic orders*. Academic Press, 2015.
- Maxim Berman, Amal Rannen Triki, and Matthew B Blaschko. The lovász-softmax loss: A tractable surrogate for the optimization of the intersection-over-union measure in neural networks. In *Proceedings of the IEEE Conference on Computer Vision and Pattern Recognition*, pages 4413–4421, 2018.
- Jeroen Bertels, David Robben, Dirk Vandermeulen, and Paul Suetens. Optimization with soft dice can lead to a volumetric bias. In *International MICCAI Brainlesion Workshop*, pages 89–97. Springer, 2019.
- Ronald Newbold Bracewell and Ronald N Bracewell. *The Fourier Transform and Its Applications*, volume 31999. McGraw-hill New York, 1986.
- Min-Te Chao and WE Strawderman. Negative moments of positive random variables. *Journal of the American Statistical Association*, 67(338):429–431, 1972.
- Olivier Chapelle and Yi Chang. Yahoo! learning to rank challenge overview. In *Proceedings of the learning to rank challenge*, pages 1–24. PMLR, 2011.
- Nontawat Charoenphakdee, Jayakorn Vongkulbhisal, Nuttapon Chairatanakul, and Masashi Sugiyama. On focal loss for class-posterior probability estimation: A theoretical perspective. In *Proceedings of the IEEE/CVF Conference on Computer Vision and Pattern Recognition*, pages 5202–5211, 2021.
- Liang-Chieh Chen, Yukun Zhu, George Papandreou, Florian Schroff, and Hartwig Adam. Encoder-decoder with atrous separable convolution for semantic image segmentation. In *Proceedings of the European Conference on Computer Vision (ECCV)*, pages 801–818, 2018.
- Stéphan Cléménçon, Gábor Lugosi, and Nicolas Vayatis. Ranking and empirical minimization of u-statistics. *Annals of Statistics*, 36(2):844–874, 2008.

- Marius Cordts, Mohamed Omran, Sebastian Ramos, Timo Rehfeld, Markus Enzweiler, Rodrigo Benenson, Uwe Franke, Stefan Roth, and Bernt Schiele. The Cityscapes dataset for semantic urban scene understanding. In *Proceedings of the IEEE Conference on Computer Vision and Pattern Recognition*, pages 3213–3223, 2016.
- Corinna Cortes and Vladimir Vapnik. Support-vector networks. *Machine Learning*, 20(3):273–297, 1995.
- David R Cox. The regression analysis of binary sequences. *Journal of the Royal Statistical Society: Series B (Methodological)*, 20(2):215–232, 1958.
- David F Crouse. On implementing 2d rectangular assignment algorithms. *IEEE Transactions on Aerospace and Electronic Systems*, 52(4):1679–1696, 2016.
- Claudia D’Ambrosio, Silvano Martello, and Michele Monaci. Lower and upper bounds for the non-linear generalized assignment problem. *Computers & Operations Research*, 120:104933, 2020.
- Jack Edmonds and Richard M Karp. Theoretical improvements in algorithmic efficiency for network flow problems. *Journal of the ACM (JACM)*, 19(2):248–264, 1972.
- M. Everingham, L. Van Gool, C. K. I. Williams, J. Winn, and A. Zisserman. The PASCAL Visual Object Classes Challenge 2012 (VOC2012) Results. <http://www.pascal-network.org/challenges/VOC/voc2012/workshop/index.html>, 2012.
- Evarist Giné and Vladimir Koltchinskii. Concentration inequalities and asymptotic results for ratio type empirical processes. *Annals of Probability*, 34(3):1143–1216, 2006.
- Tilman Gneiting and Adrian E Raftery. Strictly proper scoring rules, prediction, and estimation. *Journal of the American statistical Association*, 102(477):359–378, 2007.
- Bharath Hariharan, Pablo Arbeláez, Lubomir Bourdev, Subhransu Maji, and Jitendra Malik. Semantic contours from inverse detectors. In *2011 International Conference on Computer Vision*, pages 991–998. IEEE, 2011.
- Yili Hong. On computing the distribution function for the poisson binomial distribution. *Computational Statistics & Data Analysis*, 59:41–51, 2013.
- Shruti Jadon. Semsegloss: A python package of loss functions for semantic segmentation. *Software Impacts*, 9:100078, 2021.
- Harold W Kuhn. The hungarian method for the assignment problem. *Naval Research Logistics Quarterly*, 2(1-2):83–97, 1955.
- Tsung-Yi Lin, Priya Goyal, Ross Girshick, Kaiming He, and Piotr Dollár. Focal loss for dense object detection. In *Proceedings of the IEEE international conference on computer vision*, pages 2980–2988, 2017.
- Yi Lin. A note on margin-based loss functions in classification. *Statistics & Probability Letters*, 68(1):73–82, 2004.

- Jonathan Long, Evan Shelhamer, and Trevor Darrell. Fully convolutional networks for semantic segmentation. In *Proceedings of the IEEE Conference on Computer Vision and Pattern Recognition*, pages 3431–3440, 2015.
- Fausto Milletari, Nassir Navab, and Seyed-Ahmad Ahmadi. V-net: Fully convolutional neural networks for volumetric medical image segmentation. In *2016 Fourth International Conference on 3D Vision (3DV)*, pages 565–571. IEEE, 2016.
- Katta G Murty and Santosh N Kabadi. Some np-complete problems in quadratic and nonlinear programming. Technical report, 1985.
- Kritsana Neammanee. A refinement of normal approximation to poisson binomial. *International Journal of Mathematics and Mathematical Sciences*, 2005(5):717–728, 2005.
- John Nickolls, Ian Buck, Michael Garland, and Kevin Skadron. Scalable parallel programming with cuda: Is cuda the parallel programming model that application developers have been waiting for? *Queue*, 6(2):40–53, 2008.
- David Pollard. *Convergence of Stochastic Processes*. Springer Science & Business Media, 1984.
- Olaf Ronneberger, Philipp Fischer, and Thomas Brox. U-net: Convolutional networks for biomedical image segmentation. In *International Conference on Medical Image Computing and Computer-Assisted Intervention*, pages 234–241. Springer, 2015.
- Seyed Sadegh Mohseni Salehi, Deniz Erdogmus, and Ali Gholipour. Tversky loss function for image segmentation using 3d fully convolutional deep networks. In *International Workshop on Machine Learning in Medical Imaging*, pages 379–387. Springer, 2017.
- Xiaotong Shen. On methods of sieves and penalization. *Annals of Statistics*, 25(6):2555–2591, 1997.
- Zheng Shou, Jonathan Chan, Alireza Zareian, Kazuyuki Miyazawa, and Shih-Fu Chang. Cdc: Convolutional-de-convolutional networks for precise temporal action localization in untrimmed videos. In *Proceedings of the IEEE Conference on Computer Vision and Pattern Recognition*, pages 5734–5743, 2017.
- Carole H Sudre, Wenqi Li, Tom Vercauteren, Sebastien Ourselin, and M Jorge Cardoso. Generalised dice overlap as a deep learning loss function for highly unbalanced segmentations. In *Deep Learning in Medical Image Analysis and Multimodal Learning for Clinical Decision Support*, pages 240–248. Springer, 2017.
- Pejman Tahmasebi, Ardeshir Hezarkhani, and Muhammad Sahimi. Multiple-point geostatistical modeling based on the cross-correlation functions. *Computational Geosciences*, 16(3):779–797, 2012.
- Ambuj Tewari and Peter L Bartlett. On the consistency of multiclass classification methods. *Journal of Machine Learning Research*, 8(5), 2007.
- Nobuaki Tomizawa. On some techniques useful for solution of transportation network problems. *Networks*, 1(2):173–194, 1971.

- Guotai Wang, Maria A Zuluaga, Wenqi Li, Rosalind Pratt, Premal A Patel, Michael Aertsen, Tom Doel, Anna L David, Jan Deprest, Sébastien Ourselin, et al. Deepigeos: a deep interactive geodesic framework for medical image segmentation. *IEEE Transactions on Pattern Analysis and Machine Intelligence*, 41(7):1559–1572, 2018.
- David A Wooff. Bounds on reciprocal moments with applications and developments in stein estimation and post-stratification. *Journal of the Royal Statistical Society: Series B (Methodological)*, 47(2):362–371, 1985.
- Yang Xin, Lingshuang Kong, Zhi Liu, Chunhua Wang, Hongliang Zhu, Mingcheng Gao, Chensu Zhao, and Xiaoke Xu. Multimodal feature-level fusion for biometrics identification system on iomt platform. *IEEE Access*, 6:21418–21426, 2018.
- Tong Zhang. Statistical behavior and consistency of classification methods based on convex risk minimization. *Annals of Statistics*, 32(1):56–85, 2004.
- Hengshuang Zhao, Jianping Shi, Xiaojuan Qi, Xiaogang Wang, and Jiaya Jia. Pyramid scene parsing network. In *Proceedings of the IEEE Conference on Computer Vision and Pattern Recognition*, pages 2881–2890, 2017.